ChemPlusChem

Review
doi.org/10.1002/cplu.202400743

Chemistry Europe
European Chemical Societies Publishing

www.chempluschem.org

VIP *Very Important Paper*

Mechanistic Insight into the Thermochromic Emission of One-Dimensional Platinum(II) and Palladium(II) Complex Crystals

Masaki Yoshida*[a, b] and Masako Kato*[a]

Self-assembled Pt(II) complexes have attracted increasing interest because of their bright and colorful luminescence, as well as their stimuli-responsive properties resulting from metallophilic interactions. This review focuses on the temperature-responsive luminescent behavior (i.e., thermochromic emission) of self-assembled one-dimensional Pt(II) complexes from the viewpoint of the structure-photophysics relationship. The thermochromism of Pd(II) complexes, which have the same d^8 electronic configuration as Pt(II) complexes, is also summarized to gain a better understanding of the detailed thermochromic emissions. The mechanism of the thermochromic emissions of Pt(II) and Pd(II) complexes can be understood on the basis of two main temperature-dependent factors: (i) the energy change of the assembly, which induces excited state delocalization over two or more molecules (i.e., excited oligomers), and (ii) the thermal equilibrium between these excited oligomers. The threshold for the metal···metal distance, at which the latter factor becomes more dominant, is also discussed.

1. Introduction

Stimuli-responsive, luminescent transition-metal complexes have attracted increasing attention as luminescent sensors/probes for detecting external stimuli and environmental changes, as well as novel multifunctional optoelectronic devices.[1–6] In particular, self-assembled square-planer Pt(II) complexes have been extensively studied because their luminescent and electronic properties are drastically altered by noncovalent electronic interactions between the Pt(II) ions (i.e., metallophilic interactions).[1] Since the pioneering studies on $K_2[Pt(CN)_4]$ (known as KCP)[7] and $[Pt(NH_3)_4][PtCl_4]$ (known as Magnus' green salt),[8] the unique properties of Pt(II) complex crystals with one-dimensional metallophilic interactions have drawn significant interest. In these systems, the formation of one-dimensional chains through Pt···Pt interactions gives rise to characteristic photophysical properties,[3,4,7] chromism (stimuli-responsive and reversible color changes),[1,5,6] as well as conductivity/carrier mobility.[7–9] Thus, the crystals of Pt(II) complexes enable the creation of not only widely tunable and efficient optical materials, including organic light-emitting diodes (OLEDs),[3,4] but also smart "soft crystals" that enable the visualization of gentle external stimuli.[5]

Figure 1 presents a molecular orbital (MO) diagram of isolated and stacked Pt(II) complexes bearing aromatic chelating ligands, from which the excited states of assembled Pt(II) complexes can be understood.[1a,b] The close contact between the Pt(II) ions (typically, less than twice the van der Waals radius of Pt ($2r_w$(Pt) = 3.5 Å)[10] results in intermolecular overlap of the occupied $5d_z^2$ orbitals, thereby forming bonding dσ and antibonding dσ* orbitals (i.e., metallophilic interactions). Sim-

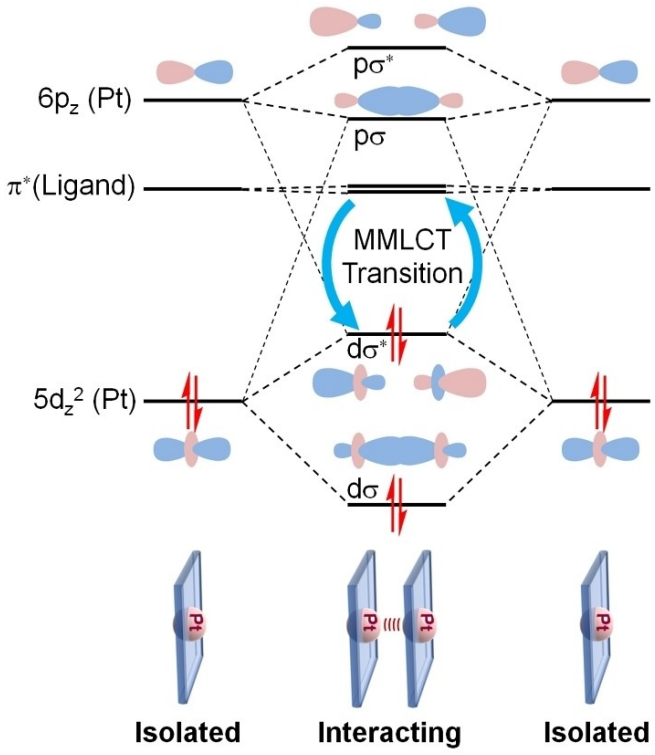

Figure 1. Schematic MO diagram of Pt(II) complexes with aromatic chelating ligand showing effective Pt···Pt interactions.

[a] *M. Yoshida, M. Kato*
Department of Applied Chemistry for Environment, School of Biological and Environmental Sciences, Kwansei Gakuin University,
1 Gakuen-Uegahara, Sanda, Hyogo 669-1330, Japan
E-mail: myoshida@chem.sci.osaka-u.ac.jp
katom@kwansei.ac.jp

[b] *M. Yoshida*
Department of Chemistry, Graduate School of Science, Osaka University,
1-1 Machikaneyama, Toyonaka, Osaka 560-0043, Japan

ilarly, bonding pσ and antibonding pσ* orbitals can be derived from the unoccupied $6p_z$ orbitals. If an aromatic chelating ligand with the appropriate π* energy level is present in this system, a charge transfer transition occurs between the dσ* and π* orbitals, termed a metal–metal-to-ligand charge transfer (MMLCT) transition. Therefore, self-assembled Pt(II) complexes with close Pt···Pt contacts are well-known to exhibit characteristic phosphorescence from the triplet state of the MMLCT (^{3}MMLCT), even if the discrete Pt(II) complexes are not emissive. Because the ^{3}MMLCT emission is derived from the newly formed excited state resulting from assembly of the Pt(II) ions, we refer to it as the "assembly-induced emission,"[1g] to distinguish it from "aggregation-induced emission," which is caused by the suppression of deactivation due to the aggregation of molecules. Although Figure 1 shows the simplest bimolecular interactions, Pt(II) complexes tend to assemble to form a one-dimensional chain through metallophilic interactions, resulting in the exciton delocalization across multiple molecules within the one-dimensional chain.[11] This exciton delocalization has recently been highlighted as a key factor in achieving highly efficient near-infrared (NIR) luminescence.[4] This is because structural displacement during excitation decreases as the number of molecules to which the exciton delocalizes increases, due to the equipartition of reorganization energy among them.[4a,11] Thus, assembled Pt(II) complexes often exhibit higher emission quantum yields than their corresponding monomers.

Because the energy level of the dσ* orbital depends on overlap of the $5d_z^2$ orbitals of the Pt(II) complex, the excited-state energy of the MMLCT changes dramatically with the Pt···Pt distance. Thus, a number of Pt(II) complexes have been reported to exhibit stimuli-responsive emission color changes driven by changes in the intermolecular arrangement due to external stimuli, including vapor (vapochromic emission), mechanical force (mechanochromic emission), and temperature (thermochromic emission). In particular, vapochromism is a representative feature of Pt(II) complexes with metallophilic interactions. In fact, the term "vapochromism" itself was originally introduced to describe the phenomenon in which double salts consisting of $[Pt(aryl\ isonitriles)_4]^{2+}$ and $[Pd(CN)_4]^{2-}$ undergo remarkable color changes upon exposure to organic vapors.[12] Since then, numerous vapochromic one-dimensional Pt(II) complexes have been reported, notably in the studies by Mann,[13] Eisenberg,[14,15] and Kato.[16,17] Based on these extensive studies, a number of review articles have been published on Pt(II) complexes exhibiting vapochromic and mechanochromic emission.[1,5] In contrast, no reviews have focused on the thermochromic properties of Pt(II) complex crystals in recent decades, despite the fact that the temperature-dependent emission behavior of Pt(II) complexes provides important information for understanding the ^{3}MMLCT excited state. In addition, the thermochromic emission of Pt(II) over a wide temperature range is interesting because of its potential applications in luminescent thermometers.

In this context, the present review focuses on the photophysical behavior of Pt(II) complexes that exhibit thermochromic shifts in the ^{3}MMLCT emission. Because thermochromic ^{3}MMLCT emission is characteristic of one-dimensional Pt(II) complexes, this review aims to provide a brief overview of the mechanisms governing the thermochromism, along with examples of such Pt(II) complexes. Of course, there are also examples of Pt(II) complexes that exhibit thermochromic emission through other mechanisms,[18,19] such as thermally activated delayed fluorescence (TADF);[18] however, this review specifically focuses on the thermochromic shift of the assembly-induced ^{3}MMLCT emission. Thus, this review begins with an introduction to mechanistic investigations of thermochromic ^{3}MMLCT emission based on photophysical, X-ray crystallographic, and theoretical studies. Thereafter, typical examples of thermochromic Pt(II) complexes reported to date are summarized from the viewpoint of the Pt···Pt distance and the emission-energy shift. Finally, these thermochromic Pt(II) complexes are compared with Pd(II) complexes, which possess the same d^8 electronic configuration.

2. Discovery and Proposed Mechanisms of Thermochromic ^{3}MMLCT Emission

Initial studies of the temperature-dependence of singlet/triplet MMLCT (^{1,3}MMLCT) excited states of Pt(II) complexes were started in the context of studies on the temperature-dependence of the dσ*→pσ transitions of a one-dimensional Pt(II) complex $K_2[Pt(CN)_4]$.[7] Paradigmatic studies of the structure–photophysical relationship of the thermochromic ^{3}MMLCT emission have been independently reported by Gray and Kato for $[Pt(bpy)Cl_2]$ and $[Pt(bpy)(CN)_2]$, respectively.[20,21] $[Pt(bpy)Cl_2]$ is known to adopt two polymorphs, a "yellow form" with a long

Masaki Yoshida received his Ph.D. degree under the supervision of Prof. Ken Sakai at Kyushu University in 2013. Then he spent a postdoctoral year in the group of Prof. Shigeyuki Masaoka at the Institute for Molecular Science in 2013. He began an academic career as an Assistant Professor at Hokkaido University in 2014, and became a Lecturer (Senior Assistant Professor) at Kwansei Gakuin University in 2022. In 2025, he was promoted to an Associate Professor at Osaka University.

Masako Kato received her Ph.D. from Nagoya University in 1986. After working at the Institute for Molecular Science and Kyoto University, she joined Nara Women's University as an Assistant Professor in 1989 and was promoted to an Associate Professor in 1996. During 1998–2001, she was also engaged in a PRESTO research. From 2006–2021, she was a Professor at Hokkaido University. Since 2021, she has been a Professor at Kwansei Gakuin University and Professor Emeritus at Hokkaido University.

Pt···Pt spacing (4.44 Å > $2r_w$(Pt)) and a "red form" with a short Pt···Pt distance (3.45 Å < $2r_w$(Pt)),[22,23] where the ^{3}MMLCT emission of the "red form" exhibits remarkable temperature-dependence.[22a] Gray et al. investigated the relationship between the Pt···Pt interaction and the ^{3}MMLCT emission of this red form of [Pt(bpy)Cl_2] (Figure 2(a)) over a wide temperature range.[20] The Pt···Pt distance decreased from 3.449(1) to 3.370(2) Å in the temperature range of 294 to 20 K ($R_{Pt\cdots Pt}$ in Figure 2(a)). Coupled with this Pt···Pt contraction, the emission maximum was red-shifted from 613 nm (300 K) to 651 nm (10 K), accompanied by an increase in the emission intensity. Kato et al. reported a similar temperature-dependence for a one-dimensional Pt(II) complex, [Pt(bpy)$(CN)_2$] (Figure 2(b)).[21] The Pt···Pt distance of this complex contracted from 3.35 Å (295 K) to 3.29 Å (15 K),[21,24] resulting in a shift of the emission maximum by ca. 50 nm, as well as an increase in the intensity, and bandwidth narrowing. Thus, contraction of the Pt···Pt distance in these complexes by less than 0.1 Å caused a significant shift in the emission maxima by ca. 1000 cm^{-1} to lower energy.

Not only due to the temperature effect but also due to the pressure effect, the ^{3}MMLCT emission energy shifts as the Pt···Pt distance changes. Valiente et al. investigated the pressure dependence of the ^{3}MMLCT emission in [Pt(bpy)Cl_2].[25] Applying hydrostatic pressure to the crystals of the red form of [Pt(bpy)Cl_2] up to 17.5 kbar resulted in a red-shift of the emission maximum to ca. 1.4×10^4 cm^{-1} (ca. 720 nm), with a linear dependence of −158 cm^{-1} bar^{-1}. Above 17.5 kbar, the red form underwent a phase transition to a different polymorphic form without Pt···Pt interactions, reducing the pressure sensitivity of the emission maximum. A direct comparison between the emission energy and the Pt···Pt distance based on X-ray crystallography under high pressure remains to be investigated; however, these results, together with thermochromism, confirm that the ^{3}MMLCT emission energy of one-dimensional Pt(II) complexes shifts in response to changes in the Pt···Pt distance.[25,26]

To date, several models have been proposed for explaining the mechanism of this thermochromic shift in the ^{3}MMLCT emission caused by the changes in the Pt···Pt distance. The simplest explanation for this phenomenon is based on overlap of the d_z^2 orbitals (Figures 1 and 3). As the Pt···Pt distance decreases with cooling, the overlap between the d_z^2 orbitals increases at low temperature, resulting in an increase in the splitting width between the dσ and dσ* orbitals. This causes a low-energy shift in the luminescence at low temperatures, as the energy difference between the dσ* and π* orbitals becomes smaller (Figure 3). However, more quantitative explanations are required to elucidate the details of the thermochromic mechanism.

The thermochromic shift of the ^{3}MMLCT emission has also been explained from the viewpoint of electrostatic coupling of the transition dipole moments (i.e., Davydov splitting). When the molecular transition dipole vectors within each stack are parallel to each other, in the point dipole approximation assuming only interactions between nearest neighbors within the stack, the low-energy shift of the transition is proportional to $|\mu|^2/R^3$,[27] where μ is the transition dipole moment in the molecule and R is the Pt···Pt spacing within the stack. As can be understood, there is a linear correlation between the emission energy-shift and both R^{-3} and $|\mu|^2$. This explanation was initially employed to account for the absorption/emission energy-shift of one-dimensional $[Pt(CN)_4]^{2-}$ salts,[7] and also

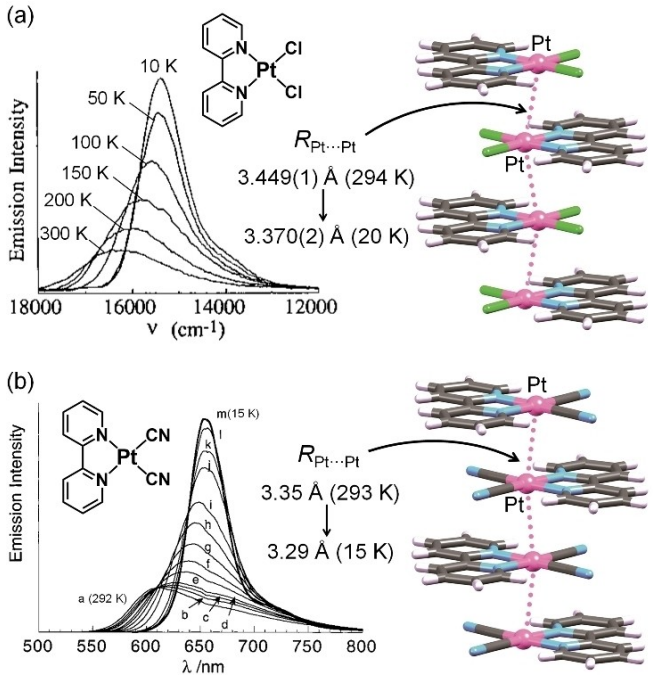

Figure 2. Stacking structures and temperature-dependence of emission spectra of (a) [Pt(bpy)Cl_2] (red form) and (b) [Pt(bpy)$(CN)_2$] in the solid state. a: 292 K; b: 260 K; c: 240 K; d: 220 K; e: 180 K; f: 160 K; g: 140 K; h: 120 K; i: 100 K; j: 60 K; k: 45 K; l: 30 K; m: 15 K. (Reprinted from Refs. [20] and [21]. Copyright 1996 and 1999 American Chemical Society).

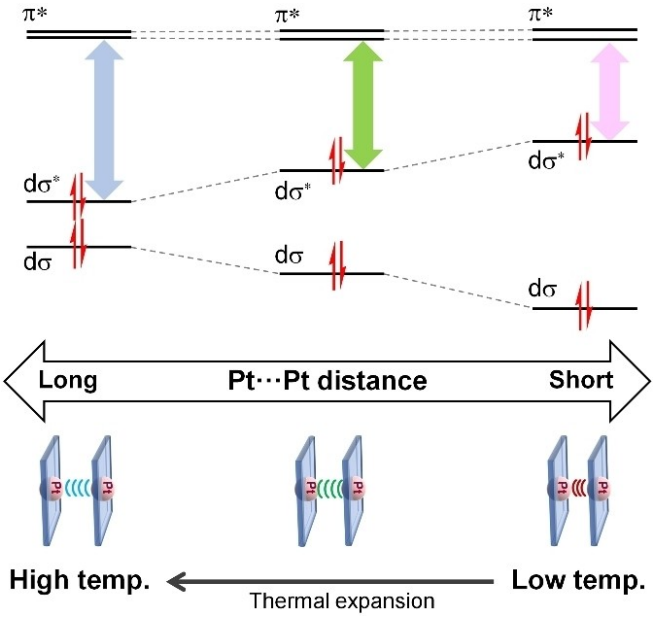

Figure 3. Schematic of thermochromic mechanism of Pt(II) complexes from the viewpoint of the dσ/dσ* splitting.

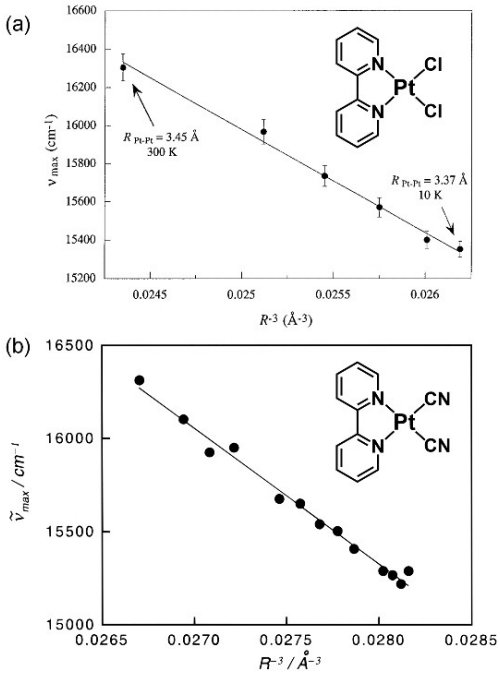

Figure 4. Plot of emission maxima vs. R^{-3} for (a) [Pt(bpy)Cl_2] (red form) and (b) [Pt(bpy)$(CN)_2$], where R is the Pt···Pt distance. (Reprinted from Refs. [20] and [21]. Copyright 1996 and 1999 American Chemical Society).

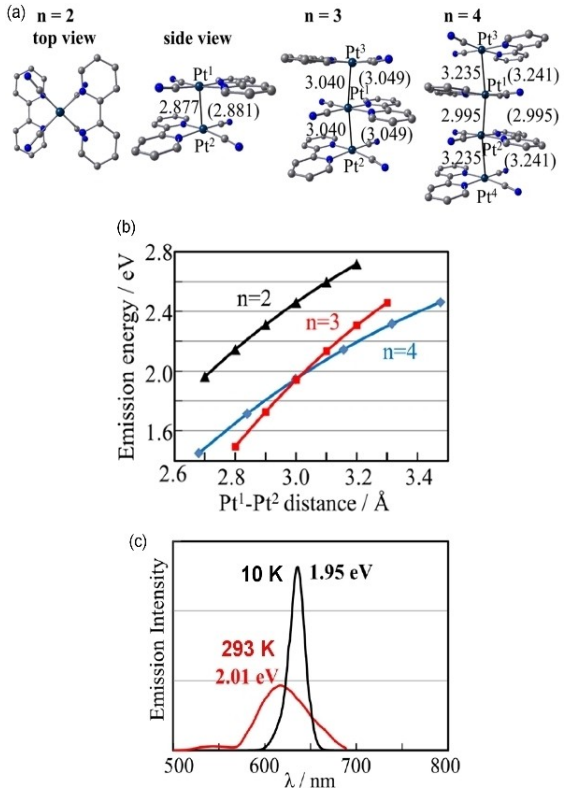

Figure 5. (a) Optimized structures of $^3\{[Pt(bpy)(CN)_2]_n\}$ (n = 2,3,4) in the ^{3}MMLCT excited state in crystal. Pt···Pt distances (in Å) are presented without parentheses for the crystal at 10 K and in parentheses for the crystal at 298 K. (b) Relationship between Pt···Pt distance and emission energy of each excited oligomer. (c) Simulated emission spectra of [Pt(bpy)$(CN)_2$] at 10 K (black) and 293 K (red). (Reprinted from Ref. [28a]. Copyright 2020 American Chemical Society).

provided good fitting results for the thermochromic shift in the ^{3}MMLCT emissions of [Pt(bpy)Cl_2] and [Pt(bpy)$(CN)_2$].[20,21] For example, the emission maxima ($\tilde{\nu}_{max}$/cm^{-1}) of [Pt(bpy)Cl_2] (red form) against R^{-3} were fitted using the following equation: $\tilde{\nu}_{max} = (29.5(55)\times10^3) - (5.4(3)\times10^5)R^{-3}$ (Figure 4(a)). Similarly, the $\tilde{\nu}_{max}$ values of [Pt(bpy)$(CN)_2$] were fitted linearly: $\tilde{\nu}_{max} = (35.7(7)\times10^3) - (7.3(3)\times10^5)R^{-3}$ (Figure 4(b)). The values of $29.5(55)\times10^3$ and $35.7(7)\times10^3$ cm^{-1} at $R^{-3} = 0$ (i.e., $R\rightarrow\infty$) are the hypothetical "monomeric ^{3}MMLCT-like" transition energies of [Pt(bpy)Cl_2] and [Pt(bpy)$(CN)_2$], respectively. However, the transition dipole moment (μ) of ^{3}MMLCT phosphorescence is significantly small, raising the question of whether this model can account for the large emission shifts of over 1000 cm^{-1} resulting from a change in the Pt···Pt distance of less than 0.1 Å. Nevertheless, this model provides a satisfactory explanation of the absorption shifts depending on the Pt···Pt distance.

Recently, Sakaki et al. proposed a new model for the thermochromic ^{3}MMLCT emission of [Pt(bpy)$(CN)_2$] based on theoretical calculations.[28] They calculated the optimized structures (Figure 5(a)) and the potential energy surfaces of the ground and excited states of the dimeric, trimeric, and tetrameric units of [Pt(bpy)$(CN)_2$]. Based on the potential energy surfaces, the ^{3}MMLCT emission maxima of each oligomeric unit were determined as a function of the Pt···Pt distance, as shown in Figure 5(b). The relationship between the calculated emission energies (E_{em}) of these excited oligomers and the Pt···Pt distance (R) was approximately represented by Eq. (1) using the empirical fitting parameters A and B:

$$E_{em} = -A \cdot \exp(-R) + B \quad (1)$$

The exponential term suggests that the emission energy of each oligomer correlates with the orbital overlap (Figure 1), given that the orbital overlap depends approximately on the exponential function of the distance. On the other hand, Sakaki pointed out the importance of the thermal population of these excited-state oligomers, which should vary with temperature. According to their calculations, the excited tetramer (i.e., $^3\{[Pt(bpy)(CN)_2]_4\}$) is 0.03 kcal mol^{-1} more stable than the excited trimer ($^3\{[Pt(bpy)(CN)_2]_3\}$) at 10 K, whereas the excited tetramer becomes 0.7 kcal mol^{-1} less stable than the excited trimer at 293 K due to expansion of the Pt···Pt distance. In addition, the excited-state dimer ($^3\{[Pt(bpy)(CN)_2]_2\}$) is significantly less stable than the excited-state trimers and tetramers. Based on Eq. (1), the probability at the Pt···Pt distance R at each temperature, and the thermal distributions of the excited states, the emission spectra of [Pt(bpy)$(CN)_2$] at 10 K and 293 K were satisfactory simulated (Figure 5(c)). Thus, this model, based on the thermal equilibrium between the excited oligomers, can successfully explain the drastic temperature-dependence of the ^{3}MMLCT emission. Notably, Chi, Chou, and co-workers recently discovered exciton delocalization over multiple Pt(II) complexes within one-dimensional chains using the pump-probe transition absorption spectroscopy.[11c,d] Therefore, the degree of this exciton delocalization could change depending on the temperature, giving rise to thermochromism of the ^{3}MMLCT emission.

These models can explain the thermochromic ^{3}MMLCT emission of one-dimensional Pt(II) complexes. As briefly noted in the Introduction, thermochromic emission is a characteristic of one-dimensional Pt(II) complexes.[14–60] In contrast, the temperature-dependence of the ^{3}MMLCT emission is typically not as significant for most dimeric Pt(II) complexes (see Sections 3 and 4),[35,48,49,61] except for a few cases, despite the metallophilic interactions in these complexes. Thus, overlap of the d_z^2 orbitals and/or coupling of the transition dipole moments between neighboring Pt(II) complexes cannot fully explain why the thermochromic shift of the ^{3}MMLCT emission of dimeric Pt(II) complexes is not very large. Therefore, in addition to the shift in the excited-state energies based on changes in the interactions between neighboring molecules, the thermal equilibrium between excited oligomers is considered to contribute to the drastic temperature-dependence of the ^{3}MMLCT emission. Of course, further experimental verification is needed to confirm this excited-state thermal equilibrium, for example, by the variable-temperature time-resolved spectroscopic studies.

3. Examples of Thermochromic ^{3}MMLCT Emission of Pt(II) Complexes

Following the discovery of thermochromism in [Pt(bpy)Cl_2] and [Pt(bpy)$(CN)_2$], a number of one-dimensional Pt(II) complexes exhibiting thermochromic ^{3}MMLCT emissions has been reported. Thus, thermochromic luminescence is recognized as a feature of ^{3}MMLCT emission, and this temperature-dependent behavior is sometimes used as evidence for the ^{3}MMLCT assignment of the emission. Table 1 and Scheme 1 summarize typical examples of one-dimensional Pt(II) complexes that exhibit thermochromic or non-thermochromic ^{3}MMLCT emissions.[20,21,16–59] The main criteria in the search for the complexes listed in Table 1 using the *ConQuest* software from the Cambridge Crystallographic Data Centre (CCDC) database are one-dimensional Pt···Pt···Pt chain structures with short Pt···Pt contacts (for this time, <3.9 Å) and aromatic chelating ligands. Important examples of such complexes are introduced in this section.

Notably, the existence of metallophilic interactions has generally been discussed on the basis of the van der Waals radius, r_w; however, the exact value of the van der Waals radius is still ambiguous.[10a,62] As shown by some examples presented in this review, even when the Pt···Pt distance is slightly longer than twice the van der Waals radius ($2r_w$(Pt) = 3.5 Å), some complexes still exhibit ^{1}MMLCT absorption and ^{3}MMLCT emission (Table 1). Therefore, the presence or absence of metallophilic interactions should be discussed based not only on the crystal structures, but also on the optical properties.

Rillema et al. reported the thermochromic ^{3}MMLCT emission of [Pt(bph)$(CO)_2$] (bph = biphenyl-2,2′-diyl),[36] which is an isoelectronic complex of [Pt(bpy)$(CN)_2$]; however, the detailed behavior of both complexes differed slightly. As shown in Figure 6, [Pt(bph)$(CO)_2$] packs in a one-dimensional columnar

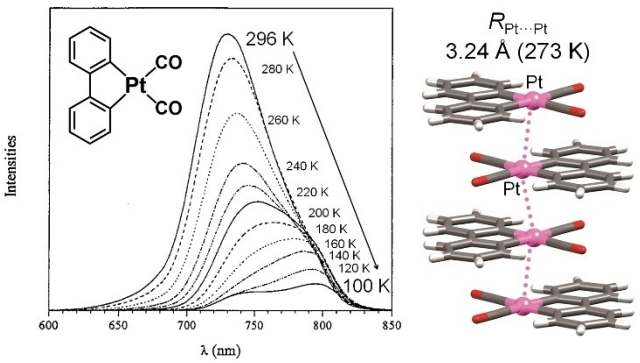

Figure 6. Stacking structure and temperature-dependence of emission spectra of [Pt(bph)$(CO)_2$] in the solid state. (Reprinted from Ref. [36]. Copyright 1998 American Chemical Society).

structure with a Pt···Pt distance of 3.24 Å at 273 K. This packing structure is isomorphous with that of [Pt(bpy)$(CN)_2$] crystal, but the Pt···Pt distance is significantly shorter than that of [Pt(bpy)$(CN)_2$] (3.35 Å at 293 K), probably due to the extremely strong σ-donating ability of the bph ligand. This complex shows intense emission at 726 nm at 296 K, and the emission maximum is red-shifted to 791 nm upon decreasing the temperature to 77 K. However, in contrast to typical cases, the emission intensity of this complex decreased with decreasing temperature, and the emission band split into two peaks at 745 nm and 791 nm at 77 K. The origin of this unusual temperature-dependent behavior is not fully understood because the crystal structure at low temperatures has not been analyzed. However, Rillema suggested that the peak-splitting at low temperatures is due to the existence of two self-trapped states from the viewpoint of the excitonic coupling model (see Section 2).[7–21] Although this complex was discovered relatively early, it is worthy of detailed investigation.

K[Pt$(CN)_2$(ppy)] (ppy = 2-phenylpyridinate), in which the anionic part is also an isoelectronic complex with [Pt(bpy)$(CN)_2$] and contains K^+ as a counter cation, displayed interesting stimuli-switchable thermochromic behavior. The vapochromic behavior of this complex was initially reported by Sicilia et al.[38] Heating the dark-purple powder of the monohydrate K[Pt$(CN)_2$(ppy)]·H_2O at 110 °C gave the yellow solid of the anhydrous K[Pt$(CN)_2$(ppy)], and when exposed to air, the color rapidly returned from yellow to purple due to moisture-adsorption (Figure 7). Although their crystal structures were not initially solved, Caliandro et al. succeeded in analyzing the crystal structures of both monohydrate and anhydrous forms.[39] For the monohydrate, the [Pt$(CN)_2$(ppy)]$^-$ anions are arranged one-dimensionally along the *c*-axis, where the electrostatic repulsion between the anionic complexes is cancelled by the K^+ ions. The intermolecular Pt···Pt distance is 3.395 Å, indicating the presence of Pt···Pt interactions. For the anhydrous species, although the parallel stacking of [Pt$(CN)_2$(ppy)]$^-$ anions along the *c*-axis was maintained, the Pt···Pt distance drastically increased to 3.9 Å (400 K) due to sliding of the complex. Thus, the Pt···Pt interactions should be negligible in the anhydrous state. This difference in Pt···Pt interactions caused the temper-

Table 1. Examples of one-dimensional, chain-like Pt(II) complexes with stacked structures connected infinitely by close Pt···Pt distances (for this time, <3.9 Å) for which the X-ray crystal structures and the temperature-dependence of the emission spectra in the solid state have been reported.

Complex	λ_{max}[a]/nm [$\tilde{\nu}_{max}$[b]/cm^{-1}]	$\Delta\tilde{\nu}_{max}$[c]/10^3 cm^{-1}	$R_{Pt\cdots Pt}$[d]/Å	Ref.
$[Pt(bpy)Cl_2]$ (red form)	613 [1.63×10^4] (300 K), 651 [1.53×10^4] (10 K)	−1.0 (300→10 K)	3.449(1) (294 K), 3.370(2) (20 K)	[20]
$[Pt(bpy)(CN)_2]$	602 [1.66×10^4] (293 K)	−1.0 (293→15 K)	3.3461(5) (295 K), 3.29 (15 K)	[21, 24]
$[Pt(i\text{-biq})(CN)_2]$	630 [1.58×10^4] (293 K)	–[e]	3.341(5) (293 K), 3.30(3) (220 K)	[21]
$[Pt(H_2dcbpy)(CN)_2]\cdot 3H_2O$	686 [1.46×10^4] (225 K), 723 [1.38×10^4] (100 K)	−0.75 (225→100 K)	3.2642(6) (225 K), 3.2161(6) (100 K)	[16, 29]
$[Pt(H_2dcphen)(CN)_2]\cdot 3H_2O$	683 [1.46×10^4] (225 K), 723 [1.38×10^4] (100 K)	−0.81 (225→100 K)	3.2768(8) (225 K), 3.2355(3) (100 K)	[29]
$[Pt(H_4dpbpy)(CN)_2]\cdot 5H_2O$	585 [1.71×10^4] (293 K)	–[f]	3.3700(9) and 3.3775(9) (200 K), 3.3403(7) and 3.3488(7) (83 K)	[30]
$[Pt(bpy)(CS_2\text{-}18\ C6\supset Na)](ClO_4)_2$	567 [1.76×10^4] (r.t.), 600 [1.67×10^4] (77 K)	−0.97 (r.t.→100 K)	3.4018(4) and 3.8474(5) (150 K)	[31]
$[Pt(bpy)(ppy)]Cl$	640 [1.56×10^4] (298 K), 675 [1.48×10^4] (77 K)	−0.81 (298→77 K)	3.6808(1) (120 K)	[32, 33]
$[Pt(bpy)(ppy)](PF_6)$	635 [1.57×10^4] (298 K), 644 [1.55×10^4] (77 K)	−0.22 (298→77 K)	3.6048(1) (93 K)	[32]
$[Pt(bpy)(gl)]\cdot 3H_2O$	663 [1.51×10^4] (298 K), 550 [1.82×10^4] (153 K)	+3.1 (298→153 K)	3.7586(5) (200 K)	[34]
$[Pt(bpy)(CC\text{-}p\text{-}pyMe)_2](PF_6)_2\cdot$dioxane	950 [1.05×10^4] (298 K), 1080 [9.26×10^3] (77 K)	−1.3 (298→77 K)	3.302(1) (100 K)	[35]
$[Pt(phen)(CC\text{-}p\text{-}pyMe)_2](PF_6)_2\cdot$MeCN	855 [1.17×10^4] (298 K), 1000 [1.00×10^4] (77 K)	−1.7 (298→77 K)	3.2398(2) (100 K)	[35]
$[Pt(bph)(CO)_2]$	726 [1.38×10^4] (296 K), 791 [1.26×10^4] (77 K)	−1.1 (296→77 K)	3.24 (273 K)	[36, 37]
$K[Pt(CN)_2(ppy)]\cdot H_2O$	745 [1.34×10^4] (298 K), 790 [1.27×10^4] (77 K)	−0.76 (298→77 K)	3.395 (293 K)	[38, 39]
$K[Pt(CN)_2(ppy)]$	636 [1.57×10^4] (298 K), 585 [1.71×10^4] (77 K)	+1.4 (298→77 K)	3.9[g] (400 K)	[38, 39]
$K[Pt(CN)_2(dFppy)]\cdot H_2O$	705 [1.42×10^4] (293 K), 800 [1.25×10^4] (77 K)	−1.7 (293→77 K)	3.3341(9) (240 K), 3.2851(9) (100 K)	[40]
$[Pt(bzq)Cl(CN^tBu)]$ (red form)	672 [1.49×10^4] (298 K), 744 [1.34×10^4] (77 K)	−1.4 (298→77 K)	3.3547(2) (173 K)	[41]
$[Pt(dFppy)Cl(CN^tBu)]$	625 [1.60×10^4] (298 K), 650 [1.54×10^4] (77 K)	−0.62 (298→77 K)	3.6876(5) and 3.8176(5) (298 K)	[42]
$[Pt(ppyCHO)Cl(CN^tBu)]\cdot 0.5$Toluene	658 [1.52×10^4] (298 K), 596 [1.68×10^4] or 706 [1.42×10^4] (77 K)[h]	–[h]	3.3620(4) and 3.8965(5) (100 K)	[42]
$[Pt(bzq)(CN)(CN^tBu)]\cdot CHCl_3$	639 [1.56×10^4] (298 K), 660 [1.52×10^4] or 720 [1.39×10^4] (77 K)[h]	–[h]	3.371(1) (100 K)	[43]
$[Pt(pbim)(pic)]\cdot 1/3c\text{-Hex}$	692 [1.45×10^4] (298 K), 721 [1.39×10^4] (77 K)	−0.58 (298→77 K)	3.4994(4) (150 K), 3.4864(4) (100 K)	[44]
$[Pt(pbim)(Fpic)]$	670 [1.49×10^4] (293 K), 710 [1.41×10^4] (77 K)	−0.84 (293→77 K)	3.4503(4) (150 K)	[45]
$[Pt(pbt)(HOpic)]\cdot 0.5CH_2Cl_2$	656 [1.52×10^4] (298 K), 680 [1.47×10^4] (77 K)	−0.54 (298→77 K)	3.3869(4) and 3.7258(4)/3.4114(4) and 3.7011(4) (100 K)	[46]
$[Pt(fppz)_2]$	625 [1.60×10^4] (298 K)	–[e]	ca. 3.1[i] (r.t)	[47]
$[Pt(Me\text{-}impy)(CN)_2]$	612 [1.63×10^4] (298 K), 691 [1.45×10^4] (77 K)	−1.9 (298→77 K)	3.2945(3) (250 K), 3.2544(2) (100 K)	[48]
$[Pt(Et\text{-}impy)(CN)_2]$	592 [1.69×10^4] (298 K), 656 [1.52×10^4] (77 K)	−1.6 (298→77 K)	3.2919(2) and 3.4579(2) (250 K), 3.2520(2) and 3.3852(2) (100 K)	[48]
$[Pt(^iPr\text{-}impy)(CN)_2]$	537 [1.86×10^4] (298 K), 555 [1.80×10^4] (77 K)	−0.60 (298→77 K)	3.3101(2) and 3.5142(2) (250 K), 3.2780(2) and 3.4588(2) (100 K)	[48]
$[Pt(^tBu\text{-}impy)(CN)_2]\cdot 3H_2O$	484 [2.07×10^4] (298 K), 472 [1.45×10^4] (77 K)	+0.5 (298→77 K)	3.4955(2) and 3.6900(2) (250 K), 3.4449(2) and 3.6257(2) (100 K)	[48]
$[Pt(Me\text{-}im\text{-}Mepy)(CN)_2]\cdot$MeOH	626 [1.60×10^4] (298 K), 692 [1.45×10^4] (77 K)	−1.5 (298→77 K)	3.2935(2) (150 K)	[49]
$[Pt(Et\text{-}im\text{-}Mepy)(CN)_2]$	579 [1.73×10^4] (298 K), 631 [1.58×10^4] (77 K)	−1.4 (298→77 K)	3.2588(8), 3.2812(9), 3.7783(9), and 3.918(1) (150 K)	[49]
$[Pt(tpy)Cl](TfO)$	600 [1.67×10^4] (298 K), 625 [1.60×10^4] (77 K)	−0.67 (298→77 K)	3.329(1) (r.t.: 283–303 K)	[50]
$[Pt(Phtpy)Cl](BF_4)\cdot$MeCN	655 [1.53×10^4] (280 K), 730 [1.37×10^4] (80 K)	−1.6 (280→80 K)	3.303(3) and 3.333(3) (153 K)	[51]
$[Pt(o\text{-}CH_3C_6H_4tpy)Cl](SbF_6)$	616 [1.62×10^4] (280 K), 673 [1.49×10^4] (80 K)	−1.4 (280→80 K)	3.368(1) (293 K)	[52]

Table 1. continued

Complex	λ_{max} [a]/nm [$\tilde{\nu}_{max}$ [b]/cm^{-1}]	$\Delta\tilde{\nu}_{max}$ [c]/10^3 cm^{-1}	$R_{Pt\cdots Pt}$ [d]/Å	Ref.
[Pt(*o*-ClC$_6$H$_4$tpy)Cl](SbF$_6$)	609 [1.64×10^4] (280 K), 642 [1.56×10^4] (80 K)	−0.84 (280→80 K)	3.374(1) and 3.513(1) (295 K), 3.311(1) and 3.550 (1) (180 K)	[53]
[Pt(*o*-ClC$_6$H$_4$tpy)(CN)](SbF$_6$)	638 [1.57×10^4] (280 K), 650 [1.54×10^4] (200 K)	−0.29 (280→80 K)	3.311(1), 3.407(1), and 3.730(1) (200 K)	[54]
[Pt(tpypyH)Cl]Cl$_2$·2H$_2$O	741 [1.35×10^4] (298 K), 779 [1.28×10^4] (77 K)	−0.69 (298→77 K)	3.3994(4) and 3.3022(7) (150 K)	[55]
[Pt(tpypyH)Cl]Cl$_2$·6H$_2$O	642 [1.35×10^4] (298 K), 658 [1.28×10^4] (77 K)	−0.38 (298→77 K)	3.385(1) and 3.705(1) (150 K)	[55]
[Pt(Nttpy)Cl](PF$_6$)$_2$	660 [1.52×10^4] (298 K), 700 [1.43×10^4] (77 K)	−0.87 (298→77 K)	3.301 and 3.360 (193 K)	[14]
[Pt(fdpb)Cl] (form G)	750 [1.33×10^4] (r.t.)	–[f]	3.4366(5) (188 K)	[56]
[Pt(dpb)(NCMe)(ClO$_4$)	755 [1.32×10^4] (298 K), 785 [1.27×10^4] (77 K)	−0.51 (298→77 K)	3.388(2) (270 K), 3.3296(3) (120 K)	[57]
[Pt(dpb)(NCMe)(TfO)	695 [1.44×10^4] (298 K), 780 [1.28×10^4] (77 K)	−1.6 (298→77 K)	3.2616(7), 3.2872(7), and 3.951(1) (200 K), 3.2333(9), 3.899(1), and 3.271(1) (120 K)	[57]
[Pt(dpb)(CNXyl)(PF$_6$) (red form)	667 [1.50×10^4] (298 K), 723 [1.38×10^4] (77 K)	−1.2 (298→77 K)	3.434 (296 K)	[58]
[Pt(bimpy)(CN)](PF$_6$)	666 [1.50×10^4] (298 K), 666 [1.50×10^4] (77 K)	±0 (298→77 K)	3.6604(3) (150 K)	[59]

[a] Emission maximum wavelength. [b] Emission maximum wavenumber. [c] Thermochromic shift of the emission maxima. [d] Pt···Pt distance. [e] In addition to the thermochromic shift of the ^{3}MMLCT band, the competitive emission from the ligand-centered $^3\pi\pi^*$ state has also been observed at low temperature. [f] Exact shift values were not documented. [g] Determined by pair distribution function (PDF) analysis. [h] Emission band shows the excitation-wavelength dependence at 77 K. [i] Half of the *c*-axis length; determined by grazing-incidence X-ray diffraction (GIXD) measurement.

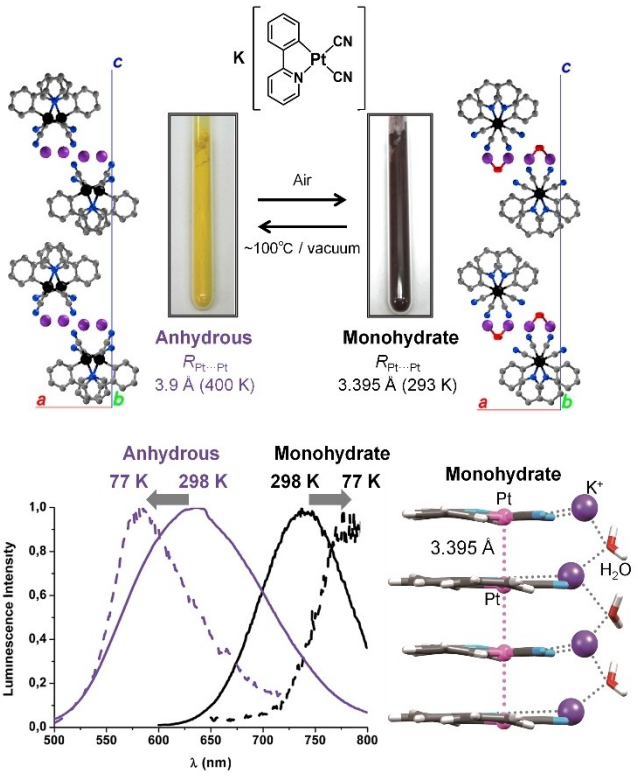

Figure 7. Packing structures, photographs, and temperature-dependence of emission spectra of the monohydrate (black lines, right) and anhydrous (purple lines, left) forms of K[Pt(CN)$_2$(ppy)] in the solid state. (Reprinted from Refs. [38] and [39]. Copyright 2008 and 2021 American Chemical Society).

ature-dependence of the monohydrate and anhydrous states to follow opposite trends. The emission band of the monohydrate was red-shifted from 745 to 790 nm upon cooling from 298 to 77 K, which is typical of the thermochromic behavior of ^{3}MMLCT emission. In contrast, the emission band of the anhydrous state sharpened at 77 K while maintaining a shorter wavelength edge, resulting in a blue-shift of the emission maximum (636 nm at 298 K to 585 nm at 77 K). Regarding the excited state properties of these forms, the emission lifetime of the anhydrous state (2.41 μs) is more than an order of magnitude longer than that of the monohydrate (0.12 μs) at 298 K,[38] suggesting that the emission origin is different from that of the ^{3}MMLCT-emissive monohydrate. The emission of the anhydrous state is suggested to be originated from the π-dimer (or excimer) emission rather than ^{3}MMLCT due to its moderate k_r value (7.1×10^4 s^{-1}),[63] which is smaller than the typical k_r values of ^{3}MMLCT emission (late 10^5 to 10^6 s^{-1}),[11a,40,48,64] as well as the longer Pt···Pt distance (3.9 Å). Thus, this complex exhibited unique switchable thermochromism upon exposure to water vapor and drying.

Recently, Kato et al. achieved systematic control of the Pt···Pt interactions and ^{3}MMLCT emission characteristics in a series of one-dimensional Pt(II) complexes based on the bulkiness of the substituent groups.[48] As shown in Figure 8, the emission colors of [Pt(CN)$_2$(R-impy)] (R-impy = 1-alkyl-3-(2-pyridyl)-1*H*-imidazolylidene) covered almost the entire visible region from red (λ_{max} = 612 nm; R = Me) to orange (λ_{max} =

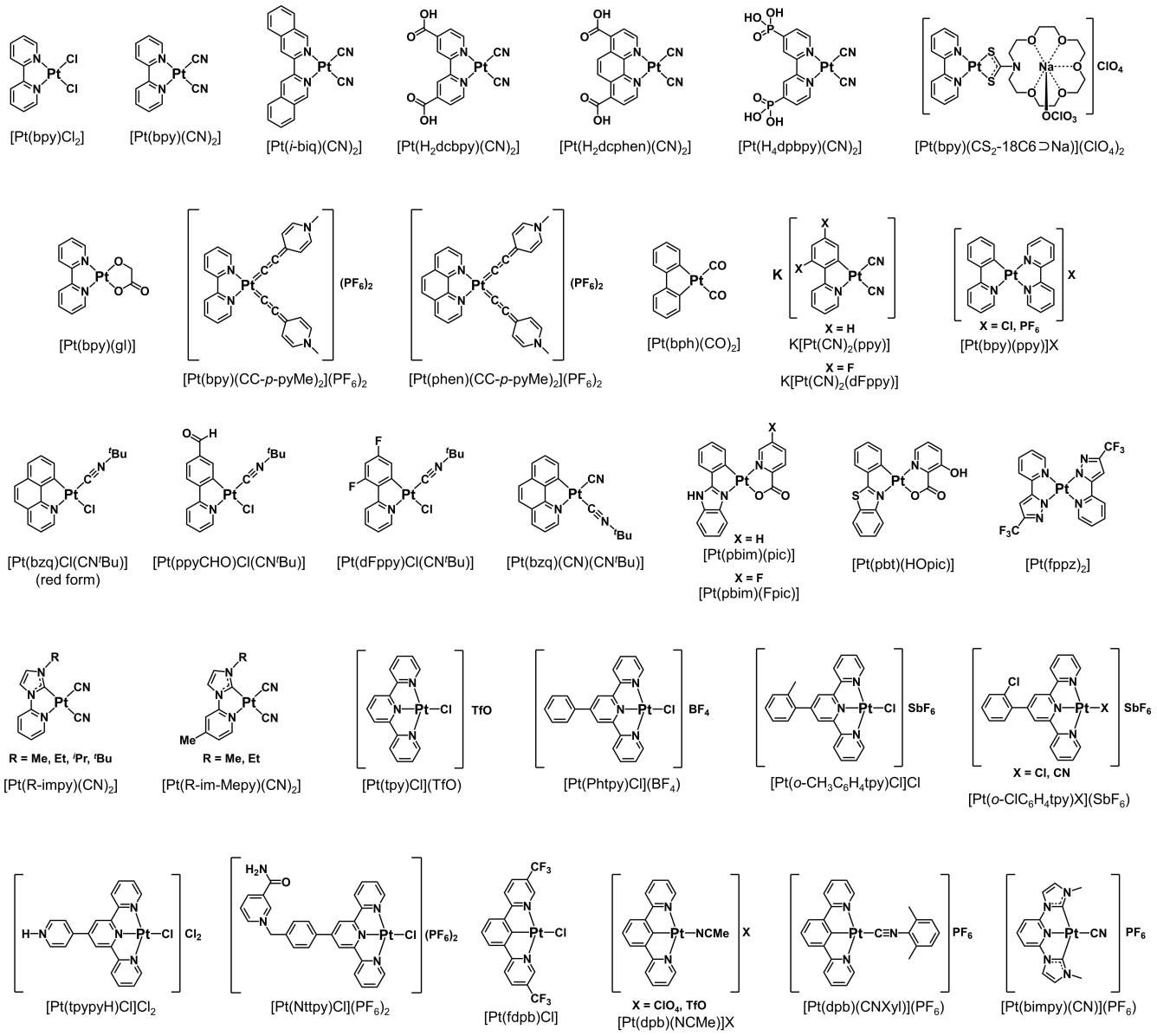

Scheme 1. Structural descriptions of Pt(II) complexes summarized in Table 1.
Abbreviations: bpy = 2,2′-bipyridine, *i*-biq = 3,3′-biisoquinoline, H_2dcbpy = 4,4′-dicarboxy-2,2′-bipyridine, H_2dcphen = 4,7-dicarboxy-1,10-phenanthroline, H_4dpbpy = 2,2′-bipyridine-4,4′-diphosphonic acid, CS_2H-18C6 = (1-aza-18-crown-6)-dithiocarbamic acid, H_2gl = glycolic acid, HCC-*p*-pyMe$^+$ = 1-methyl-4-ethynylpyridinium, H_2bph = biphenyl, Hppy = 2-phenyipyridine, HdFppy = 2-(2,4-difluorophenyl)pyridine, Hbzq = benzo[*h*]quinoline, ppyCHO = 4-(2-pyridyl)-benzaldehyde, Hpbim = 2-phenylbenzimidazole, Hpic = α-picolinic acid, H(Fpic) = 5-fluoro-α-picolinic acid, Hpbt = 2-phenylbenzothiazole, H(HOpic) = 3-hydroxy-α-picolinic acid, Hfppz = 3-(trifluoromethyl)-5-(2-pyridyl)-pyrazole, R-impyH$^+$ = 3-alkyl-1-(2-pyridyl)-1*H*-imidazolium, R-im-MepyH$^+$ = 3-alkyl-1-(4-methyl-(2-pyridinyl))-1*H*-imidazolium, tpy = 2,2′:6′,2″-terpyridine, Phtpy = 4′-phenyl-2,2′:6′,2″-terpyridine, *o*-$CH_3C_6H_4$tpy = 4′-(2‴-methylphenyl)-2,2′:6′,2″-terpyridine, *o*-ClC_6H_4tpy = 4′-(2‴-chlorophenyl)-2,2′:6′,2″-terpyridine, tpypy = 2,2′:6′,2″-terpyridine-4′,4‴-pyridine, Nttpy = 4′-(*p*-nicotinamide-*N*-methylphenyl)-2,2′:6′,2″-terpyridine, Hfdpb = 1,3-bis(5-trifluoromethyl-2-pyridyl)benzene, dpb = 1,3-di(2-pyridyl)benzene, CNXyl = 2,6-xylyl isocyanide, bimpy = 2,6-bis(3-methyl-1*H*-imidazol-2-ylidene)pyridine.

592 nm; R = Et), green (λ_{max} = 537 nm; R = ^{i}Pr), and finally blue (λ_{max} = 484 nm; R = ^{t}Bu) at 298 K. This is due to the change in the Pt···Pt distance depending on the bulkiness of the substituent groups. All the complexes exhibited very high emission quantum yields (Φ) of 0.51–0.81 with sub-microsecond emission lifetimes (τ) of 0.29–0.88 μs at 298 K. These high emission quantum yields can be attributed to both exciton delocalization and the strong ligand field of the carbene ligand. Importantly, although the shortest Pt···Pt distances of the Me, Et, and ^{i}Pr-substituted complexes were rather similar (3.2817(2), 3.2762(2), and 3.2956(2) Å, respectively), the emission maxima shifted drastically depending on the bulkiness of the substituent. Because the average Pt···Pt distance increased in accordance with increasing bulkiness of the substituents, the Pt···Pt electronic interactions should be delocalized over the one-dimensional chain (see Section 2) rather than over the neighboring two molecules. Notably, not only the emission color but also the thermochromic shift of the emission was changed by

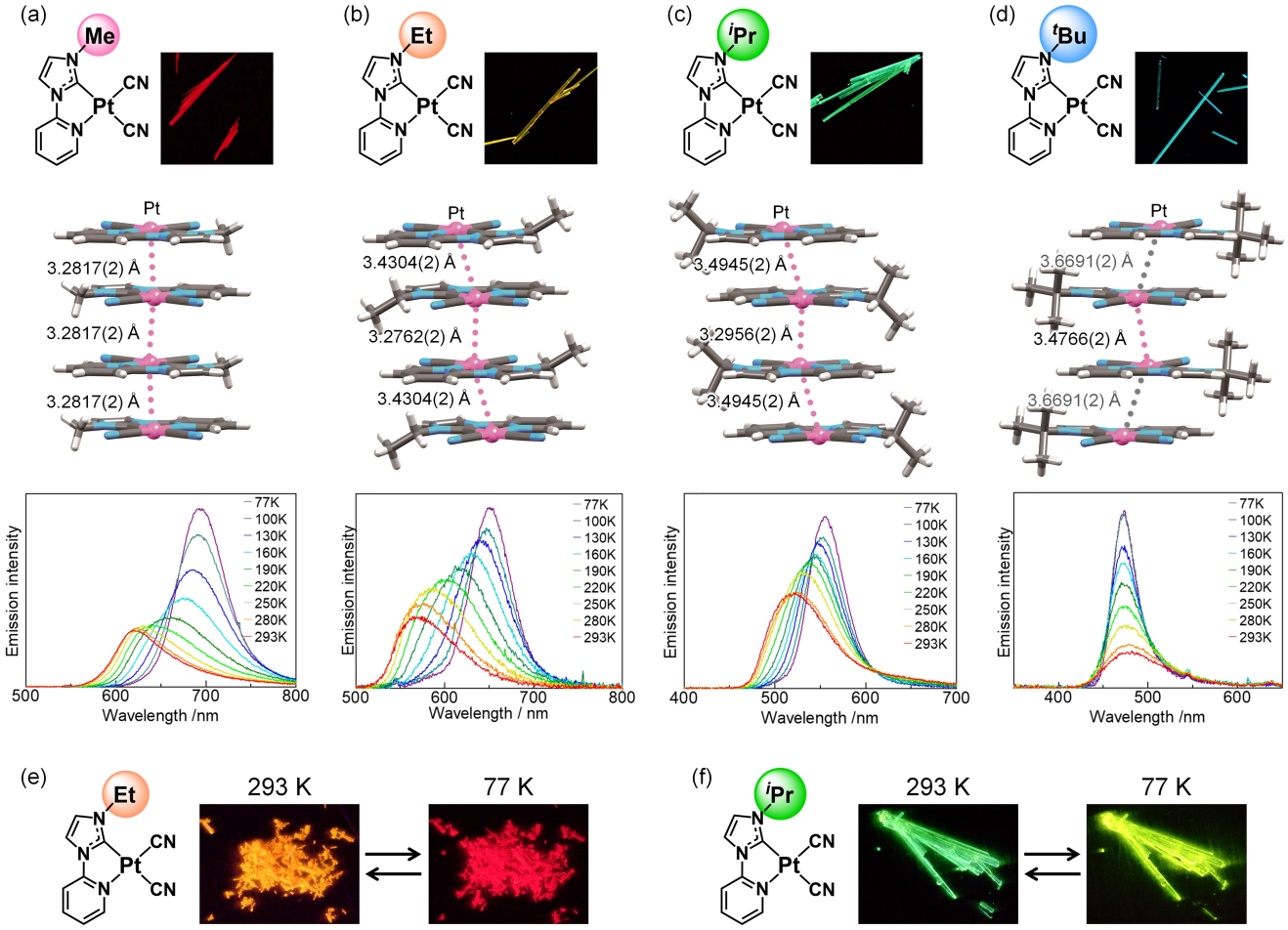

Figure 8. (a–d) Stacking structures at 200 K, photographs, and temperature dependence of emission spectra of a series of $[Pt(CN)_2(R\text{-impy})]$ (R = Me (a), Et (b), ^{i}Pr (c), and ^{t}Bu (d)) in the solid state. (e,f) Photographs of the thermochromic emission of (e) $[Pt(CN)_2(Et\text{-impy})]$ and (f) $[Pt(CN)_2(^{i}Pr\text{-impy})]$. (Reprinted from ref. [48] for (a–d). Copyright 2020 Wiley-VCH GmbH)

the substituent groups. The Me-, Et-, and ^{i}Pr-substituted complexes exhibited a typical emission shift with temperature (Figure 8(e, f)), whereas no spectral shift was observed for the ^{t}Bu-substituted complex over a wide temperature range (Figure 8(d)). This difference can be understood from the thermal equilibrium model of delocalized excited states (see Section 2). Among the complexes, one of the two inequivalent Pt···Pt distances of the ^{t}Bu-substituted complex (3.6691(2) Å) is slightly longer than twice the van der Waals radius of Pt (3.5 Å), indicating that the ^{3}MMLCT emission of the ^{t}Bu complex originates primarily from dimeric interactions with negligible thermal equilibrium. The maximum emission energies of the complexes were plotted against the average Pt···Pt distance at each temperature (R_{ave}; Figure 9). The data clearly showed that the limit of the Pt···Pt interaction is in the region of 3.5–3.6 Å, indicating a threshold Pt···Pt distance of ca. $2r_w$(Pt), which allows delocalization of the excited states in the one-dimensional Pt···Pt chain.

The importance of the delocalization of excited states across multiple molecules for achieving large thermochromic ^{3}MMLCT emissions has also been suggested by other researchers. For example, Lu et al. reported differences in the temperature

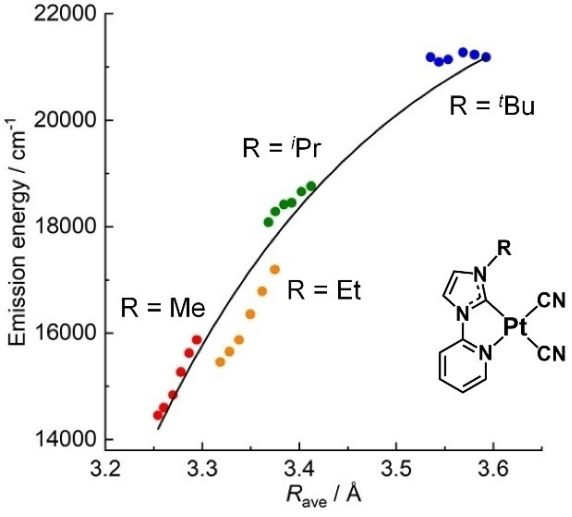

Figure 9. Correlation between maximum emission energy and Pt···Pt distance (R_{ave}) for $[Pt(CN)_2(R\text{-impy})]$ (R = Me (red), Et (orange), ^{i}Pr (green), and ^{t}Bu (blue)) in the range of 100–250 K. The black, solid line is the least-squares fit based on the equation: $E\ [cm^{-1}] = -(4.15\times10^{9})\ \exp(-R_{ave}\ [Å]/0.250) + (2.36\times10^{4})$ (Reprinted from Ref. [48]. Copyright 2020 Wiley-VCH GmbH).

response between isomers of Pt(II) complexes bearing *N*-heterocyclic allenylidene (NHA) ligands, as part of their interest in controlling the luminescence and assembly/aggregation of Pt(II) complexes.[35] As shown in Figure 10(a), the cationic part of $[Pt(bpy)(CC\text{-}p\text{-}pyMe)_2](PF_6)_2$ ($H(CC\text{-}p\text{-}pyMe)^+$ = 1-methyl-4-ethynylpyridinium) stacked one-dimensionally with a Pt···Pt distance of 3.302(1) Å at 100 K. Owing to these one-dimensional Pt···Pt interactions, as well as the σ-donating/π-accepting abilities of the NHA ligand, the *p*-isomer, $[Pt(bpy)(CC\text{-}p\text{-}pyMe)_2](PF_6)_2$, exhibited ^{3}MMLCT emission in the NIR region of 950 nm at 298 K, and this emission maximum was further red-shifted to 1080 nm at 77 K. In contrast, the packing structures and temperature-dependence of the emissions of the *o*- and *m*-isomers were found to be entirely distinct from those of the *p*-isomer. The *o*-isomer formed a dimeric structure with a Pt···Pt distance of 3.3384(3) Å, which was further loosely stacked (Pt···Pt of 4.3476(4) Å) in the crystal (Figure 10(b)). Therefore, the emission of the *o*-isomer was moderately red-shifted from 650 nm (298 K) to 690 nm (77 K). For the *m*-isomer, the Pt atoms between the two molecules interacted weakly (3.5004(3) Å; Figure 10(c)), forming a discrete dimer without interaction with the adjacent dimer, resulting in a minimal temperature-dependence of the emission energy (628 nm at 298 K, 638 nm at 77 K). Thus, delocalization of the excited state over multiple molecules can induce a drastic thermochromic phenomenon owing to the thermal equilibrium between the excited oligomers.

As discussed above, in most cases, a contraction of the Pt···Pt distance at low temperatures should result in a red-shift of the ^{3}MMLCT emission of one-dimensional Pt(II) complexes; however, alternative factors may sometimes be the primary cause of this phenomenon. Chuang, Chi, Chou, and co-workers investigated the detailed emission behavior of a vapor-deposited thin film of $[Pt(fppz)_2]$ (fppz = 3-(trifluoromethyl)-5-(2-pyridyl)-pyrazolate), revealing an additional factor influencing the thermochromic emission.[47] This thin film was initially reported for use in an efficient OLED device with an extremely high external quantum efficiency (EQE) of 38.8%.[65] As is characteristic of typical one-dimensional Pt(II) complexes, a temperature-dependent shift of the ^{3}MMLCT emission band of $[Pt(fppz)_2]$ was observed above 125 K (Figure 11(a)) Notably, in this temperature range, a relatively slow intermolecular structural relaxation during excitation (τ = 41 ns at 298 K) was detected prior to the ^{3}MMLCT emission (τ = 341 ns at 298 K). Grazing-incidence X-ray diffraction (GIXD) analysis of the thin film of $[Pt(fppz)_2]$ revealed anisotropic lattice contraction of the crystal in the direction of the *a*-axis upon cooling (Figure 11(b)). However, in contrast to the usual cases, this *a*-axis corresponds to the interchain direction (Figure 11(c)), while the *c*-axis can be assigned to the direction of the one-dimensional Pt···Pt chain. Thus, the interchain contraction at low temperature is a critical factor in the thermochromic red-shift of the ^{3}MMLCT emission in this case, and the observed slow structural relaxation with τ = 41 ns is attributable to the interchain motion during excitation. Given this result, we may also have to consider the interchain motion of one-dimensional Pt(II) chains, particularly obliquely stacked chains with weak interchain interactions.[66]

Based on these reports, the temperature-dependence of the ^{3}MMLCT emission is usually small when the Pt···Pt distance is longer than approximately 3.5–3.6 Å,[35,42,48,49,61] but there are some exceptions. For example, the cationic moiety of [Pt(bpy)(ppy)]Cl stacked in a typical one-dimensional columnar

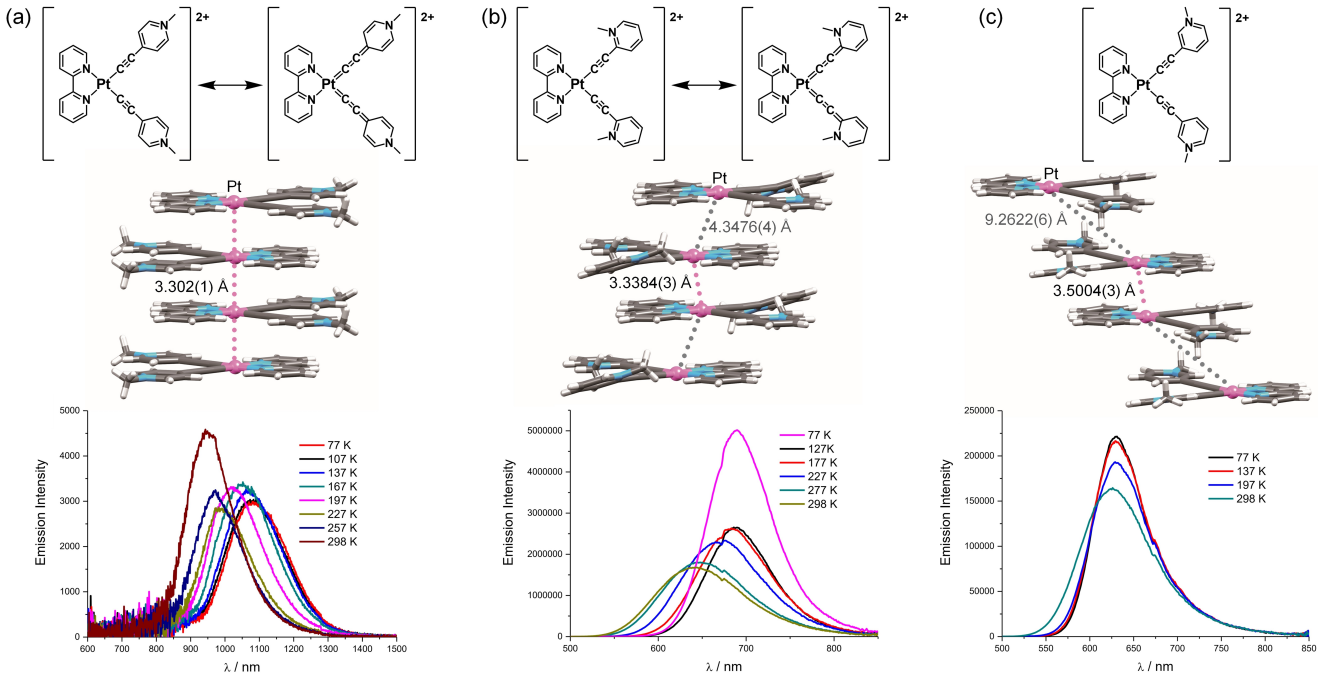

Figure 10. Stacking structures at 100 K, photographs, and temperature-dependence of emission spectra of (a) *p*-, (b) *o*-, and (c) *m*-isomers of $[Pt(bpy)(CC\text{-}pyMe)_2](PF_6)_2$ in the solid state. (Reprinted from Ref. [35]. Copyright 2023 American Chemical Society).

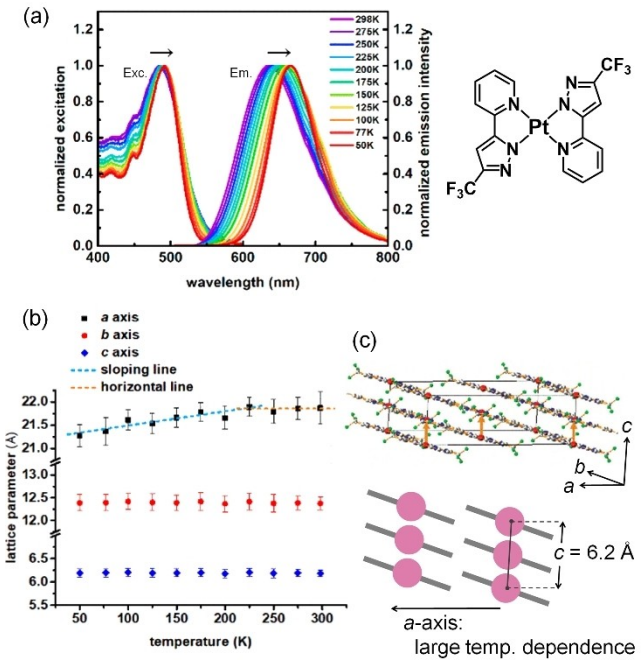

Figure 11. Temperature-dependence of (a) normalized excitation and emission spectra and (b) lattice parameters of vapor-deposited [Pt(fppz)$_2$] thin film. (c) Packing structure of [Pt(fppz)$_2$] in thin film, determined by GIXD measurement. (Reprinted from Refs. [47, 65]. Copyright 2016 WILEY-VCH Verlag GmbH & Co. KGaA, and 2021 American Chemical Society).

structure, although the Pt···Pt distance of 3.6808(1) Å is slightly longer than 3.5–3.6 Å.[33] Despite this relatively long Pt···Pt distance, the ^{3}MMLCT emission band of this complex was significantly red-shifted from 640 nm (298 K) to 675 nm (77 K).[32] The unusually large thermochromic shift considering the long Pt···Pt distance can be understood by comparison with its derivative. In fact, the fluorinated derivative with a bulky anion, [Pt(bpy)(dFppy)](BPh$_4$) (dFppy = 2-(2,4-difluorophenyl)pyridinate),[67] formed a dimeric structure instead of the one-dimensional chain, and its longer intra-dimer Pt···Pt distance of 3.755 Å indicates very weak Pt···Pt interactions even within the dimer. However, the ^{3}MMLCT emission of [Pt(bpy)(dFppy)](BPh$_4$) still showed thermochromism (570 nm (297 K)→586 nm (77 K)), driven by shortening of the intra-dimer Pt···Pt distance at low temperature.[67] In other words, these [Pt(bpy)(ppy)]-type complexes tend to exhibit a relatively large ^{3}MMLCT thermochromic shift even in the dimeric state, despite the relatively longer Pt···Pt distances, in contrast with the ^{3}MMLCT emissions of typical dimeric Pt(II) complexes.[35,42,48,49,61] The unusually large thermochromism of [Pt(bpy)(ppy)]-type complexes may be caused by the large structural relaxation during excitation, facilitated by significant π-π interactions between the aromatic ligands.

Although most thermochromic Pt(II) complexes exhibit a red-shift of the emission at low temperatures, some Pt(II) complexes with relatively longer Pt···Pt distances show an interesting thermochromic blue-shift of the emission with decreasing temperature. An example is the previously described K[Pt(CN)$_2$(ppy)] (anhydrous; Pt···Pt distance of 3.9 Å; Figure 7), for which the dimer emission is blue-shifted upon cooling.[38] Fujihara et al. reported similar behavior for [Pt(bpy)(gl)] (gl = glycolate).[34] Among the three isolated polymorphs of the complex, the emission maximum of the trihydrate "red form" exhibited a blue-shift from 663 to 550 nm upon cooling from 298 to 153 K, while maintaining the shorter-wavelength edge of the emission band (Figure 12). Notably, the long Pt···Pt intermolecular distance of 3.786(5) Å suggests very weak (or negligible) Pt···Pt interactions, at least in the ground state. Thus, the emission of this crystal can be attributed to the excimer (or, based on the solid-state absorption spectrum, the π-dimer-type) emission. Therefore, the excited-state structural relaxation of the excimer should be suppressed at lower temperatures, thereby causing a blue-shift in the emission upon cooling.

In addition to simple one-dimensional Pt(II) complexes, heterometallic chains composed of Pt(II) and other metal ions have also been demonstrated a thermochromic red-shift of the emission band.[68–70] For example, Martín, Moreno, and co-workers reported the thermochromic behavior of a heterometallic Tl(I)/Pt(II) one-dimensional chain {[Tl(Me$_2$CO)][Pt(bzq)(C$_6$F$_5$)$_2$]} (Figure 13; bzq = benzo[*h*]quinolinate), along with its vapochromic and mechanochromic properties.[68] Tl(I) ions tend to interact with Pt(II) through dative bonds because the occupied 6 s and empty 6p$_z$ orbitals of Tl(I) largely overlap with the occupied 5d$_{z^2}$ and empty 6p$_z$ orbitals of Pt(II), respectively.[71] Indeed, this chain is constructed with short Pt–Tl distances (2.9301(3), 2.9609(3), 2.9945(3), and 3.0666(3) Å), which are shorter than the sum of the van der Waals radii of Pt and Tl (r_w(Pt) = 1.75 Å, r_w(Tl) = 1.96 Å).[7a] This Tl(I)/Pt(II) chain exhibited bright orange-red phosphorescence (610 nm, 1.64×10^4 cm^{-1}), which was significantly red-shifted upon cooling to 77 K (685 nm, 1.46×10^4 cm^{-1}). Thus, the energy-shifts of the excited states and the thermal equilibria between the excited states play significant roles in the thermochromic emission of heterometallic chains in addition to Pt(II) chains.

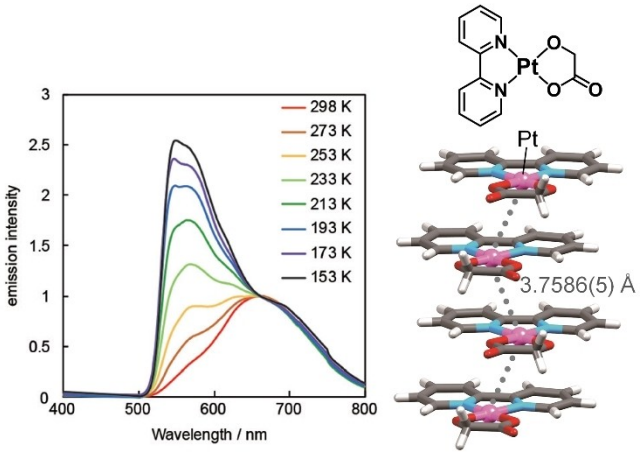

Figure 12. Stacking structure at 200 K and temperature-dependence of emission spectra of the red form (trihydrate form) of [Pt(bpy)(gl)] in the solid state. (Reprinted from Ref. [34]. Copyright 2020 the Royal Society of Chemistry).

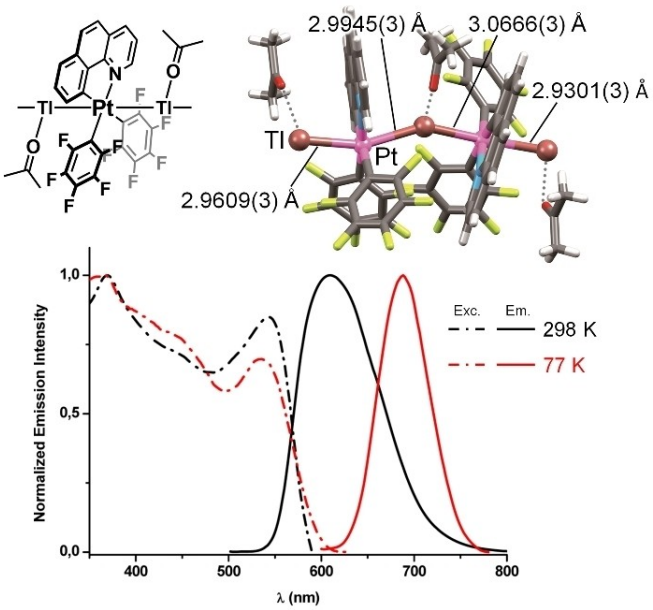

Figure 13. Chain structure and emission (solid lines) and excitation spectra (broken lines) of {[Tl(Me$_2$CO)][Pt(bzq)(C$_6$F$_5$)$_2$]} at 298 K (black) and 77 K (red) in the solid state. (Reprinted from Ref. [68]. Copyright 2015 American Chemical Society).

4. Temperature-Dependent ^{3}MMLCT Emissions of Pd(II) Complexes: Similarity to and Difference from those of Pt(II) Congeners

To gain a better understanding of the thermochromic ^{3}MMLCT emissions, understanding the relationship between the types of metal ion species and their excited states based on metallophilic interactions is crucial. Therefore, the last part of this review presents the temperature-dependence of the ^{3}MMLCT emissions of Pd(II) complexes, which have the same d^8 electronic configuration as Pt(II) complexes, and discuss the implications of the observed differences.

In contrast to Pt(II) complexes, Pd(II) complexes rarely exhibit assembly-induced ^{3}MMLCT emission,[72] despite having the same d^8 electronic configuration. This is mainly due to the following two reasons: (i) The 4d$_z^2$ orbital of Pd is smaller and less diffused than the 5d$_z^2$ orbital of Pt, which results in less favorable intermolecular overlap of the orbitals. (ii) The weaker ligand fields of Pd(II) complexes compared to those of Pt(II) complexes give rise to non-radiative deactivation through readily accessible metal-centered ^{3}d-d excited states. Therefore, introducing a very strong ligand field that makes the Pd(II) center more electron-rich and suppresses deactivation via the ^{3}d-d excited states can effectively overcome this problem. In 2018, Che et al. reported, for the first time, the ^{3}MMLCT-emissive one-dimensional Pd(II) complex [Pd(pbpy)(CNXyl)](PF$_6$)$_2$ (Hpbpy = 6-phenyl-2,2′-bipyridine, CNXyl = 2,6-xylyl isocyanide), where the Pd···Pd distances of 3.3732(4) and 3.3449(4) Å (at 100 K) are slightly longer than twice the van der Waals radius of Pd ($2r_w$(Pd) = 3.26 Å), but short enough for the metal centers to interact.[73] This complex exhibited a broad ^{3}MMLCT emission band with an emission maximum around 540 nm (Φ = ca. 0.45). In the same year, Lu et al. also succeeded in obtaining the one-dimensional Pd(II) complex [Pd(pbpy)(CCim)](PF$_6$)$_2$ (HCCim$^+$ = 2-ethynyl-1,3-dimethyl-1*H*-imidazolium; Figure 14(a)) with very short Pd···Pd contacts of 3.295(2) and 3.298(2) Å (at 100 K), which exhibited vapo-, mechano-, and thermochromic ^{3}MMLCT emissions.[74] Its emission maximum was observed at 695 nm (Φ = 0.43), which is in a longer wavelength region than that of the aforementioned complex. To date, Che,[73,75] Lu,[74,76] Strassert,[77] Li,[78] Kinzhalov,[79] and Kato[40,59] successfully developed Pd(II) complexes that unambiguously exhibit assembly-induced ^{3}MMLCT and related emissions.

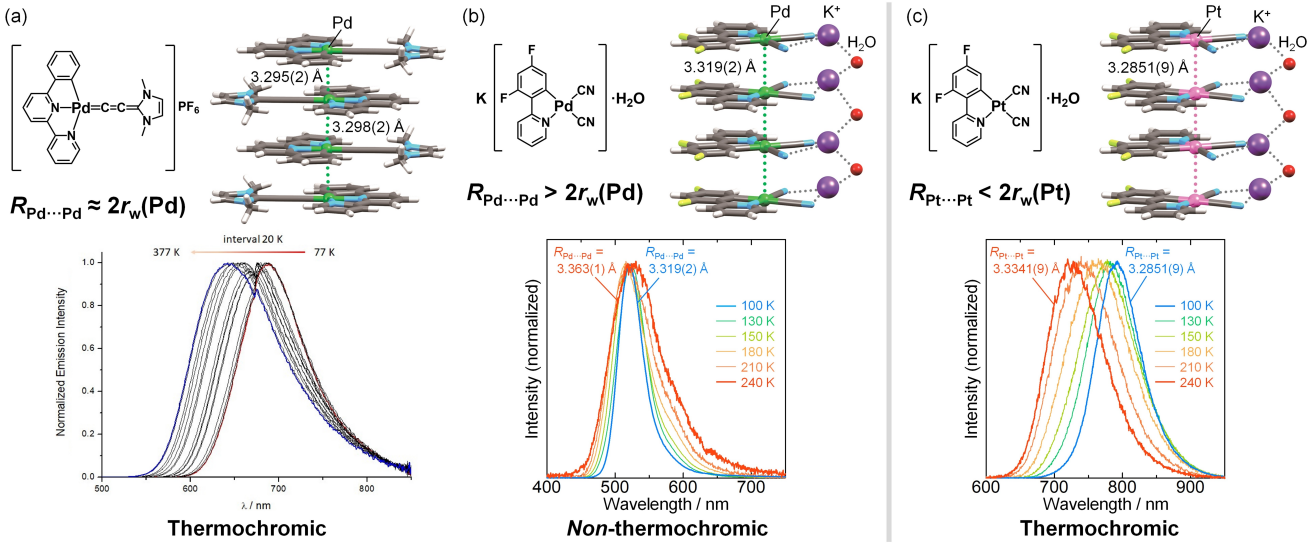

Figure 14. Stacking structures at 100 K and of temperature-dependence of emission spectra of (a) [Pd(pbpy)(CCim)](PF$_6$)$_2$, (b) K[Pd(CN)$_2$(dFppy)]·H$_2$O, and (c) K[Pt(CN)$_2$(dFppy)]·H$_2$O in the solid state. (Reprinted from Refs. [74a] and [40]. Copyright 2018 and 2024 the Royal Society of Chemistry).

Among the ^{3}MMLCT-emissive one-dimensional Pd(II) complexes, some exhibit temperature-dependent emission. As briefly mentioned above, the red powder of [Pd(pbpy)(CCim)](PF$_6$)$_2$, as reported by Lu, exhibited ^{3}MMLCT emission at 695 nm at 298 K, and this emission band underwent a significant red-shift at low temperatures (Figure 14(a)).[74] The thermochromic emission of this complex is similar to that of the typical one-dimensional Pt(II) complexes mentioned above (see Sections 2 and 3). In contrast, the authors recently reported the non-thermochromic ^{3}MMLCT emission of a one-dimensional Pd(II) complex.[40] The ^{3}MMLCT emission band of K[Pd(CN)$_2$(dFppy)]·H$_2$O shifted only slightly with temperature, with emission maxima ranging from 534 nm at 293 K to 520 nm at 77 K (Figure 14(b)), despite the contraction of the Pd···Pd distance from 3.363(1) Å (240 K) to 3.319(2) Å (100 K). Instead, the emission intensity of K[Pd(CN)$_2$(dFppy)]·H$_2$O was drastically enhanced to approximately unity upon cooling ($\Phi < 0.01$ at 293 K to $\Phi = 0.92$ at 77 K). Notably, the emission of the crystallographically isomorphous Pt(II) chain, K[Pt(CN)$_2$(dFppy)]·H$_2$O, showed a drastic thermochromic shift from 705 to 800 nm in the same temperature range (Figure 14(c) and Table 1). Thus, the lack of thermochromism of K[Pd(CN)$_2$(dFppy)]·H$_2$O may reflect the difference in the delocalization of the ^{3}MMLCT excited state between this Pd(II) chain and the corresponding Pt(II) chain.

This difference can be discussed from the viewpoint of the distance between the metals and the van der Waals radii (r_w(M), M = Pt or Pd) (Figure 15). As discussed above in relation to Figure 9, the threshold of the Pt···Pt distances is plausibly around the 2r_w(Pt) value, which allows delocalization of the excited states in the one-dimensional Pt···Pt chain.[48] Not limited to Pt(II) complexes, most of the ^{3}MMLCT-emissive d^8 metal complexes that exhibit large thermochromism are one-dimensional chains with M···M distances shorter than 2r_w(M) (or pseudo-one-dimensional chains comprising trimers, tetramers, or pentamers). Thus, considering Sakaki's model (Section 2),[28] if the M···M distance is comparable to or sufficiently shorter than 2r_w(M), a large thermochromic shift is caused by thermal equilibrium between the excited oligomers (Figure 15(a)). In contrast, the excited states of non-(or slightly−)thermochromic one-dimensional chains are localized to two neighboring molecules, which are not in thermal equilibrium with the excited states of the further extended oligomers (Figure 15(b)). Notably, the van der Waals radii of Pt and Pd (r_w(Pt) and r_w(Pd), respectively) were originally proposed based on the change in the absorption of the crystals of [M(Hdmg)$_2$] (H$_2$dmg = dimethylglyoxime),[10b] but in fact, this absorption band can be assigned to the one-dimensionally delocalized dσ*(M···M)→pσ(M···M) type transitions.[80] In other words, the 2r_w(Pt) and 2r_w(Pd) values indicate that the M···M distances are sufficient to facilitate the extension of the electronically delocalized excited state across multiple molecules (i.e., excited oligomer formation) in a one-dimensional chain. Of course, the exact value of the threshold of M···M distance responsible for the thermal equilibrium between the excited oligomers would depend on the ligand structures, the stacking modes, and the tilt angle of the Pt(II) coordination plane from the stacking axis. Nevertheless, the value of 2r_w(M) can serve as a reference point for a preliminary discussion of the excited states in one-dimensional Pt(II) and Pd(II) complexes.

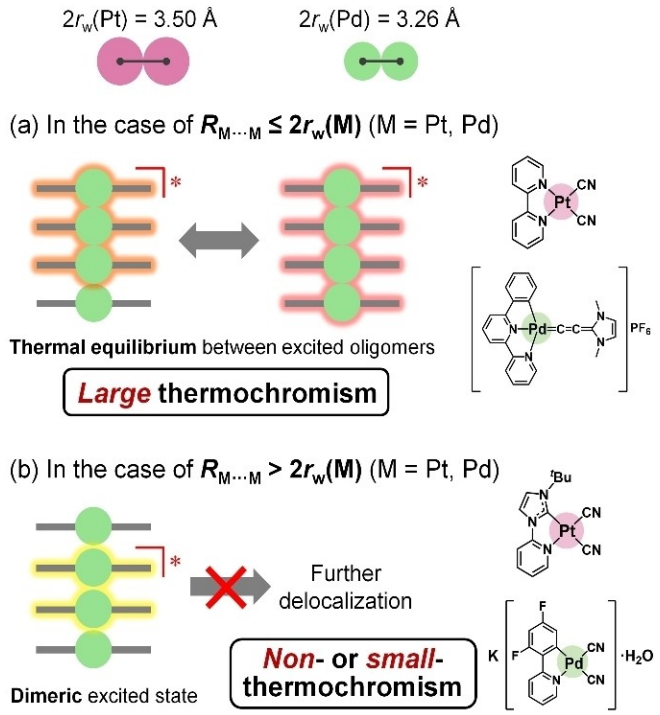

Figure 15. Suggested differences in the delocalization of the ^{3}MMLCT excited state of one-dimensional Pt(II) and Pd(II) complexes in cases where the M···M distance is (a) less than or (b) greater than twice the van der Waals radius.

This conclusion reveals not only the cause of the thermochromic emission shift, but also the cause of the difference in thermal emission quenching between Pt(II) and Pd(II) complexes. As noted in Introduction, molecular displacement during excitation could be suppressed by exciton delocalization across multiple molecules.[11] On the other hand, unlike the Pt(II) analogue, the ^{3}MMLCT excited state of K[Pd(CN)$_2$(dFppy)]·H$_2$O was localized over only two adjacent molecules.[40] As a result, its emission underwent drastic thermal quenching ($\Phi < 0.01$ at 293 K, $\Phi = 0.92$ at 77 K) through thermal deformation into a more stable, highly distorted, and non-emissive conformation. Such drastic and rapid thermal quenching has not been observed in the Pt(II) analogue K[Pt(CN)$_2$(dFppy)]·H$_2$O, suggesting the importance of the extension of the exciton delocalization. Because the spin-orbit coupling of the Pd(II) complex is weaker than that of the Pt(II) complex, the radiative rate constant of K[Pd(CN)$_2$(dFppy)]·H$_2$O ($k_r = 6.6\times10^4$ s^{-1} at 77 K)[40] was relatively small; therefore, the emission of K[Pd(CN)$_2$(dFppy)]·H$_2$O was significantly influenced by structural distortion compared to that of K[Pt(CN)$_2$(dFppy)]·H$_2$O.

The last part of this review focuses on whether the formation of excited oligomers differs significantly for thermochromic and non-thermochromic Pd(II) complexes. For this purpose, a comparison of the M···M distances and ^{3}MMLCT emission energies of [M(pbpy)(CCim)](PF$_6$)$_2$, [M(pbpy)(CNXyl)](PF$_6$)$_2$, K[M(CN)$_2$(dFppy)]·H$_2$O, and [M**LF**] (H$_2$**LF** = *N*,*N*-di-[6-(2,6-difluoropyridin-3-yl)-4-methoxypyridin-2-yl]-4-hex-

ylaniline), in which the Pd(II) complex and the corresponding Pt(II) complex are crystallographically isomorphic, is presented (Figure 16(a–c)). Among these complexes, [Pt**LF**] and [Pd**LF**], reported by Strassert and co-workers,[77b] formed isomorphic dimers with close M···M distances in the crystal. Thus, their emission unambiguously originates from the ^{3}MMLCT localized on the dimers (Figure 16(c)). The shift in the dimeric emission energy of [Pt**LF**] relative to that of [Pd**LF**] ($\Delta\tilde{\nu}_{max}$ (Pd–Pt)) was approximately 2.0×10^3 cm^{-1}. This value is similar to the shift in the calculated vertical excitation energy of the *dimeric models* of K[M(CN)$_2$(dFppy)]·H$_2$O ($\Delta\tilde{\nu}_{maxx}$ (Pd–Pt) = 2.2×10^3 cm^{-1}) (Figure 16(d)).[40] However, the actual ^{3}MMLCT emission energy of K[Pt(CN)$_2$(dFppy)]·H$_2$O was red-shifted by 4.5×10^3 cm^{-1} compared to that of K[Pd(CN)$_2$(dFppy)]·H$_2$O (Figure 16(b)), suggesting a difference in the degree of excited-state delocalization for the Pt(II) versus Pd(II) complexes. Therefore, K[Pt(CN)$_2$(dFppy)]·H$_2$O should form excited oligomers, whereas such an extension of the excited state is negligible for K[Pd(CN)$_2$(dFppy)]·H$_2$O, as discussed in relation to Figures 14 and 15. This conclusion is further supported by the comparison between [M(pbpy)(CCim)](PF$_6$)$_2$ ($\Delta\tilde{\nu}_{max}$ (Pd–Pt) = 2.3×10^3 cm^{-1})[76c] and [M(pbpy)(CNXyl)](PF$_6$)$_2$ ($\Delta\tilde{\nu}_{max}$ (Pd–Pt) = 4.6×10^3 cm^{-1})[73,81] (Figure 16(a, b)). Given that the Pd···Pd distances of [Pd(pbpy)(CNXyl)](PF$_6$)$_2$ are slightly longer than 2r_w(Pd), in contrast with those of [Pd(pbpy)(CCim)](PF$_6$)$_2$, the excited electron density of [Pd(pbpy)(CNXyl)](PF$_6$)$_2$ may be less delocalized compared to that of [Pd(pbpy)(CCim)](PF$_6$)$_2$. Because both of the corresponding Pt(II) complexes should possess largely delocalized excited states within the one-dimensional chain, the differences in the excited state delocalization and excitation energies of [Pd(pbpy)(CCim)](PF$_6$)$_2$ and [Pt(pbpy)(CCim)](PF$_6$)$_2$ are considered to be smaller than those of [M(pbpy)(CNXyl)](PF$_6$)$_2$ cases. Overall, for both one-dimensional Pt(II) and Pd(II) chains, the excited states are more delocalized when the M···M distance is less than ca. 2r_w(M), leading to large thermochromism based on thermal equilibrium between the excited oligomers, although the exact value of the threshold distance should depend on the complexes.

5. Summary and Outlook

This review summarized studies on crystalline, one-dimensional Pt(II) and Pd(II) complexes exhibiting thermochromic ^{3}MMLCT emission. Although the thermochromic shift in the emission is recognized as a characteristic feature of ^{3}MMLCT-emissive Pt(II) complexes, this behavior has not been comprehensively reviewed in recent decades. A survey of these studies revealed that the thermochromic mechanism of one-dimensional Pt(II) and Pd(II) complexes can be understood based on two main temperature-dependent factors: (i) the energy change of the ^{3}MMLCT excited state[20,21,27,67] and (ii) thermal equilibrium between the excited oligomers.[28,40,48] In particular, the latter mechanism is effective when the metal···metal distance is comparable to or less than approximately twice the van der Waals radius, allowing a drastic thermochromic shift in the emission induced by a change in the Pt···Pt distance of less than 0.1 Å. Of course, further experimental verification is needed to determine how many molecules are actually involved in the thermal equilibrium in the excited state. Notably, the molecular design based on these mechanisms is expected to lead to the development of thermochromic and multifunctional d^8 (e.g., Pt(II), Pd(II), Ni(II), Rh(I), and Au(III)) and d^{10} (e.g., Au(I), Ag(I), and Cu(I)) metal complexes with metallophilic interactions. For example, Au(I) complexes are also well-known to exhibit assembly-induced emission based on Au···Au interactions

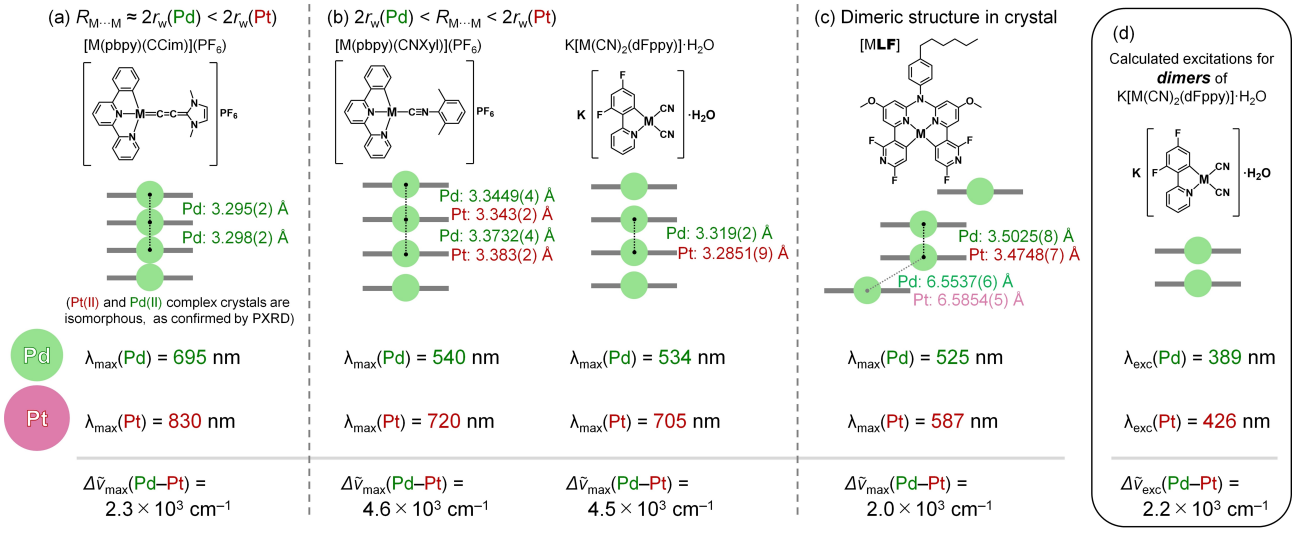

Figure 16. (a–c) M···M distances, ^{3}MMLCT emission maximum wavelengths, and energy differences between emission maxima for crystallographically isomorphic Pt(II) and Pd(II) complexes, in which (a) indicates the case where the M···M distances are shorter than or comparable to both 2r_w(Pt) and 2r_w(Pd), (b) indicates the case where the M···M distances are between 2r_w(Pt) and 2r_w(Pd), and (c) indicates the case where the complexes form dimers in the crystals. Although the single-crystal X-ray structure of [Pt(pbpy)(CCim)](PF$_6$)$_2$ has not been reported, powder X-ray diffraction (PXRD) measurements revealed the isomorphic nature of the Pt(II) and Pd(II) complex crystals.[76c] (d) Calculated ^{1}MMLCT vertical transition energies for the dimeric units of K[M(CN)$_2$(dFppy)]·H$_2$O (M = Pt, Pd).

(aurophilic interactions);[2,82] thus, the findings presented here should be useful for understanding and designing vapo-, mechano-, and thermo-responsive one-dimensional Au(I) complexes. Moreover, these findings are expected to provide insight into the pressure dependence of the emission properties of Au(I) chains.[83] Some Ni(II) complexes exhibiting assembly-induced emission based on metallophilic interactions have recently been reported;[84] therefore, it would be interesting to explore the application of Ni(II) complexes in this system. In addition, because one-dimensional chains with such metallophilic interactions are known to exhibit carrier mobility,[7–9,85] such solid-state properties are expected to be associated with thermochromism. These complexes are also expected to be applied as luminescent thermometers that visualize a wide range of temperatures, from around the liquid-helium temperature to approximately 100 °C. Although the thermochromism of one-dimensional Pt(II) chains has long been known, a deep understanding of this phenomenon will expand the rich chemistry of smart optoelectronic materials and multi-stimuli-responsive soft crystals.

Acknowledgements

The authors acknowledge the financial support of JSPS KAKENHI (grant numbers JP21K05094, JP22H02098, JP23 K23366, and JP24K08455), and also the Hyogo Science and Technology Association and the Kyoto Technoscience Center.

Conflict of Interests

The authors declare no conflict of interest.

Keywords: Assembly-induced emission · Metallophilic interactions · Palladium complexes · Platinum complexes · Thermochromism

[1] a) M. Kato, *Bull. Chem. Soc. Jpn.* **2007**, *80*, 287–294; b) O. S. Wenger, *Chem. Rev.* **2013**, *113*, 3686–3733; c) Q. Zhao, F. Li, C. Huang, *Chem. Soc. Rev.* **2010**, *39*, 3007–3030; d) M. Mauro, A. Aliprandi, D. Septiadi, N. S. Kehr, L. De Cola, *Chem. Soc. Rev.* **2014**, *43*, 4144–4166; e) A. Aliprandi, D. Genovese, M. Mauro, L. De Cola, *Chem. Lett.* **2015**, *44*, 1152–1169; f) K. Li, G. S. M. Tong, Q. Wan, G. Cheng, W.-Y. Tong, W.-H. Ang, W.-L. Kwong, *Chem. Sci.* **2016**, *7*, 1653–1673; g) M. Yoshida, M. Kato, *Coord. Chem. Rev.* **2018**, *356*, 101–115; h) M. Chaaban, C. Zhou, H. Lin, B. Chyi, B. Ma, *J. Mater. Chem. C* **2019**, *7*, 5910–5924; i) M. Yoshida, M. Kato, *Coord. Chem. Rev.* **2020**, *408*, 213194; j) B. Li, Z. Liang, H. Yan, Y. Li, *Mol. Syst. Des. Eng.* **2020**, *5*, 1578–1605; k) S. Horiuchi, K. Umakoshi, *Chem. Rec.* **2021**, *21*, 469–479; l) A. Ito, M. Iwamura, E. Sakuda, *Coord. Chem. Rev.* **2022**, *467*, 214610; m) S.-Y. Yang, Y. Chen, R. T. K. Kwok, J. W. Y. Lam, B. Z. Tang, *Chem. Soc. Rev.* **2024**, *53*, 5366–5393.

[2] a) H. Schmidbaur, A. Schier, *Chem. Soc. Rev.* **2012**, *41*, 370–412; b) C. Jobbágy, A. Deák, *Eur. J. Inorg. Chem.* **2014**, 4434–4449; c) R. Li, F.-F. Xu, Z.-L. Gong, Y.-W. Zhong, *Inorg. Chem. Front.* **2020**, *7*, 3258–3281; d) N. Mirzadeh, S. H. Privér, A. J. Blake, H. Schmidbaur, S. K. Bhargava, *Chem. Rev.* **2020**, *120*, 7551–7591; e) M. Jin, H. Ito, *J. Photochem. Photobiol. C* **2022**, *51*, 100478; f) B. Yang, S. Yan, Y. Zhang, F. Feng, W. Huang, *Dalton Trans.* **2024**, *53*, 5320–5341.

[3] a) J. A. G. Williams, S. Develay, D. L. Rochester, L. Murphy, *Coord. Chem. Rev.* **2008**, *252*, 2596–2611; b) T. Strassner, *Acc. Chem. Res.* **2016**, *49*, 2680–2689; c) C. Cebrián, M. Mauro, *Beilstein J. Org. Chem.* **2018**, *14*, 1459–1481; d) Y. Zhang, Y. Wang, J. Song, J. Qu, B. Li, W. Zhu, W.-Y. Wong, *Adv. Opt. Mater.* **2018**, *6*, 1800466; e) Q.-C. Zhang, H. Xiao, X. Zhang, L.-J. Xu, Z.-N. Chen, *Coord. Chem. Rev.* **2019**, *378*, 121–133; f) V. W.-W. Yam, A. S.-Y. Law, *Coord. Chem. Rev.* **2020**, *414*, 213298; g) A. Nitti, D. Pasini, *Adv. Mater.* **2020**, *32*, 1908021.

[4] a) Y.-C. Wei, K.-H. Kuo, Y. Chi, P.-T. Chou, *Acc. Chem. Res.* **2023**, *56*, 689–699; b) P. L. dos Santos, P. Stachelek, Y. Takeda, P. Pander, *Mater. Chem. Front.* **2024**, *8*, 1731–1766; c) M. Wałęsa-Chorab, *J. Photochem. Photobiol. C* **2024**, *59*, 100664; d) C. Zhang, Y. Fang, D. He, K. Xu, Y. Bian, Y. Li, M. Peng, W. Xiong, *Top. Curr. Chem.* **2024**, *382*, 31.

[5] a) M. Kato, H. Ito, M. Hasegawa, K. Ishii, *Chem. Eur. J.* **2019**, *25*, 5105–5112; b) M. Kato, M. Yoshida, Y. Sun, A. Kobayashi, *J. Photochem. Photobiol. C* **2022**, *51*, 100477; c) M. Kato, *IUCrJ* **2024**, *11*, 442–452.

[6] a) X. Zhang, B. Li, Z.-H. Chen, Z.-N. Chen, *J. Mater. Chem.* **2012**, *22*, 11427–11441; b) X. Zhang, Z. Chi, Y. Zhang, S. Liu, J. Xu, *J. Mater. Chem. C* **2013**, *1*, 3376–3390; c) A. Kobayashi, M. Kato, *Eur. J. Inorg. Chem.* **2014**, 4469–4483; d) V. W.-W. Yam, V. K.-M. Au, S. Y.-L. Leung, *Chem. Rev.* **2015**, *115*, 7589–7728; e) A. J. McConnell, C. S. Wood, P. P. Neelakandan, J. R. Nitschke, *Chem. Rev.* **2015**, *115*, 7729–7793; f) Y. Sagara, S. Yamane, M. Mitani, C. Weder, T. Kato, *Adv. Mater.* **2016**, *28*, 1073–1095; g) P. Xue, J. Ding, P. Wang, R. Lu, *J. Mater. Chem. C* **2016**, *4*, 6688–6706; h) M. A. Soto, R. Kandel, M. J. MacLachlan, *Eur. J. Inorg. Chem.* **2021**, 894–906; i) M. Sadeghian, M. G. Haghighi, E. Lalinde, M. T. Moreno, *Coord. Chem. Rev.* **2022**, *452*, 214310; j) K. Shinozaki, *Dalton Trans.* **2024**, *53*, 15782–15786.

[7] a) G. Gliemann, H. Yersin, *Struct. Bond.* **1985**, *62*, 87–153; b) P. Day, *J. Am. Chem. Soc.* **1975**, *97*, 1588–1589; c) H. Yersin, G. Gliemann, *Ann. N. Y. Acad. Sci.* **1978**, *313*, 539–559; d) T. W. Thomas, A. E. Underhill, *Chem. Soc. Rev.* **1972**, *1*, 99–120.

[8] a) M. Atoji, J. W. Richardson, R. E. Rundle, *J. Am. Chem. Soc.* **1957**, *79*, 3017–3020; b) L. Atkinson, P. Day, R. J. P. Williams, *Nature* **1968**, *218*, 668–669; c) W. Caseri, *Platinum Met. Rev.* **2004**, *48*, 91–100; d) E.-G. Kim, K. Schmidt, W. R. Caseri, T. Kreouzis, N. Stingelin-Stutzmann, J.-L. Brédas, *Adv. Mater.* **2006**, *18*, 2039–2043.

[9] a) K. Sakai, E. Ishigami, Y. Konno, T. Kajiwara, T. Ito, *J. Am. Chem. Soc.* **2002**, *124*, 12088–12089; b) C. H. Hendon, A. Walsh, N. Akiyama, Y. Konno, T. Kajiwara, T. Ito, H. Kitagawa, K. Sakai, *Nat. Commun.* **2016**, *7*, 11950.

[10] a) A. Bondi, *J. Phys. Chem.* **1964**, *68*, 441–451; b) C. V. Banks, D. W. Barnum, *J. Am. Chem. Soc.* **1958**, *80*, 3579–3582.

[11] a) K. T. Ly, R.-W. Chen-Cheng, H.-W. Lin, Y.-J. Shiau, S.-H. Liu, P.-T. Chou, C.-S. Tsao, Y.-C. Huang, Y. Chi, *Nat. Photonics* **2017**, *11*, 63–68; b) S. F. Wang, Y. Yuan, Y.-C. Wei, W.-H. Chan, L.-W. Fu, B.-K. Su, I.-Y. Chen, K.-J. Chou, P.-T. Chen, H.-F. Hsu, C.-L. Ko, W.-Y. Hung, C.-S. Lee, P.-T. Chou, Y. Chi, *Adv. Funct. Mater.* **2020**, *30*, 2002173; c) Y.-C. Wei, S. F. Wang, Y. Hu, L.-S. Liao, D.-G. Chen, K.-H. Chang, C.-W. Wang, S.-H. Liu, W.-H. Chan, J.-L. Liao, W.-Y. Hung, T.-H. Wang, P.-T. Chen, H.-F. Hsu, Y. Chi, P.-T. Chou, *Nat. Photonics* **2020**, *14*, 570–577; d) S.-F. Wang, B.-K. Su, X.-Q. Wang, Y.-C. Wei, K.-H. Kuo, C.-H. Wang, S.-H. Liu, L.-S. Liao, W.-Y. Hung, L.-W. Fu, W.-T. Chuang, M. Qin, X. Lu, C. You, Y. Chi, P.-T. Chou, *Nat. Photonics* **2022**, *16*, 843–850.

[12] C. C. Nagel, U.S. Patent 4,834,909 (**1989**).

[13] a) C. L. Exstrom, J. R. Sowa Jr., C. A. Daws, D. Janzen, K. R. Mann, *Chem. Mater.* **1995**, *7*, 15–17; b) C. E. Buss, C. E. Anderson, M. K. Pomije, C. M. Lutz, D. Britton, K. R. Mann, *J. Am. Chem. Soc.* **1998**, *120*, 7783–7790; c) S. M. Drew, D. E. Janzen, C. E. Buss, D. I. MacEwan, K. M. Dublin, K. R. Mann, *J. Am. Chem. Soc.* **2001**, *123*, 8414–8415; d) S. M. Drew, D. E. Janzen, K. R. Mann, *Anal. Chem.* **2002**, *74*, 2547–2555.

[14] T. J. Wadas, Q.-M. Wang, Y.-J. Kim, C. Flaschenreim, T. N. Blanton, R. Eisenberg, *J. Am. Chem. Soc.* **2004**, *126*, 16841–16849.

[15] a) P. Du, J. Schneider, W. W. Brennessel, R. Eisenberg, *Inorg. Chem.* **2008**, *47*, 69–77; b) A. Han, P. Du, Z. Sun, H. Wu, H. Jia, R. Zhang, Z. Liang, R. Cao, R. Eisenberg, *Inorg. Chem.* **2014**, *53*, 3338–3344.

[16] M. Kato, S. Kishi, Y. Wakamatsu, Y. Sugi, Y. Osamura, T. Koshiyama, M. Hasegawa, *Chem. Lett.* **2005**, *34*, 1368–1369.

[17] a) S. Kishi, M. Kato, *Mol. Cryst. Liq. Cryst.* **2002**, *379*, 303–308; b) M. Kato, A. Omura, A. Toshikawa, S. Kishi, Y. Sugimoto, *Angew. Chem. Int. Ed.* **2002**, *41*, 3183–3185.

[18] a) P. Pander, A. V. Zaytsev, A. Sil, J. A. G. Williams, P.-H. Lanoe, V. N. Kozhevnikov, F. B. Dias, *J. Mater. Chem. C* **2021**, *9*, 10276–10287; b) A. Russegger, S. M. Fischer, A. C. Debruyne, H. Wiltsche, A. D. Boese, R. I. Dmitriev, S. M. Borisov, *ACS Appl. Mater. Interfaces* **2024**, *16*, 11930–11943; c) G. S. Lee, K. M. Hwang, I. Kang, S. H. Hong, S. Kim, Y. Jeong, R. Elumalai, S.-B. Ko, T. Kim, Y.-H. Kim, *Adv. Opt. Mater.* **2025**, *13*, 2402230.

[19] a) T. Ogawa, M. Yoshida, H. Ohara, A. Kobayashi, M. Kato, *Chem. Commun.* **2015**, *51*, 13377–13380; b) T. Ogawa, W. M. C. Sameera, M. Yoshida, A. Kobayashi, M. Kato, *Dalton Trans.* **2018**, *47*, 5589–5594.
[20] W. B. Connick, L. M. Henling, R. E. Marsh, H. B. Gray, *Inorg. Chem.* **1996**, *35*, 6261–6265.
[21] M. Kato, C. Kosuge, K. Morii, J. S. Ahn, H. Kitagawa, T. Mitani, M. Matsushita, T. Kato, S. Yano, M. Kimura, *Inorg. Chem.* **1999**, *38*, 1638–1641.
[22] a) V. H. Houlding, V. M. Miskowski, *Coord. Chem. Rev.* **1991**, *111*, 145–152; b) V. M. Miskowski, V. H. Houlding, *Inorg. Chem.* **1989**, *28*, 1529–1533; c) R. H. Herber, M. Croft, M. J. Coyer, B. Bilash, A. Sahiner, *Inorg. Chem.* **1994**, *33*, 2422–2426.
[23] a) R. S. Osborn, D. Rogers, *J. Chem. Soc. Dalton Trans.* **1974**, 1002–1004; b) A. J. Cnaty, B. W. Skelton, P. R. Traill, A. H. White, *Aust. J. Chem.* **1992**, *45*, 417–422; c) A. L. Grzesiak, A. J. Matzger, *Inorg. Chem.* **2007**, *46*, 453–457.
[24] W. B. Connick, L. M. Henling, R. E. March, *Acta Crystallogr. Sect. B* **1996**, *52*, 817–822.
[25] a) O. S. Wenger, S. García-Revilla, H. U. Güdel, H. B. Gray, R. Valiente, *Chem. Phys. Lett.* **2004**, *384*, 190–192; b) R. Valiente, J. M. García-Lastra, P. García-Fernández, S. García-Revilla, O. S. Wenger, *Eur. J. Inorg. Chem.* **2007**, 5735–5742.
[26] A. Rodrigue-Witchel, D. L. Rochester, S.-B. Zhao, K. B. Lavelle, J. A. G. Williams, S. Wang, W. B. Connick, C. Reber, *Polyhedron* **2016**, *108*, 151–155.
[27] a) D. P. Craig, P. C. Hobbins, *J. Chem. Soc.* **1955**, 539–548; b) D. Fox, O. Schnepp, *J. Chem. Phys.* **1955**, *23*, 767–775.
[28] a) M. Nakagaki, S. Aono, M. Kato, S. Sakaki, *J. Phys. Chem. C* **2020**, *124*, 10453–10461; b) J.-J. Zheng, S. Sakaki, *J. Photochem. Photobiol. C* **2022**, *51*, 100482.
[29] Y. Shigeta, A. Kobayashi, T. Ohba, M. Yoshida, T. Matsumoto, H.-C. Chang, M. Kato, *Chem. Eur. J.* **2016**, *22*, 2682–2690.
[30] A. Kobayashi, N. Yamamoto, Y. Shigeta, M. Yoshida, M. Kato, *Dalton Trans.* **2018**, *47*, 1548–1556.
[31] B.-C. Tzeng, C.-C. Liao, P.-Y. Jung, S.-Y. Chen, B.-J. Sun, W.-C. Cheng, A. H. H. Chang, G.-H. Lee, *Inorg. Chem.* **2023**, *62*, 916–929.
[32] H. Matsukawa, M. Yoshida, T. Tsunenari, S. Nozawa, A. Sato-Tomita, Y. Maegawa, S. Inagaki, A. Kobayashi, M. Kato, *Sci. Rep.* **2019**, *9*, 15151.
[33] J. Yang, L. Sun, L. Hao, G.-G. Yang, Z.-C. Zou, Q. Cao, L.-N. Jia, Z.-W. Mao, *Chem. Commun.* **2019**, *55*, 11191–11194.
[34] K. Ohno, M. Komuro, T. Sugaya, A. Nagasawa, T. Fujihara, *Dalton Trans.* **2020**, *49*, 1873–1882.
[35] J. Lin, F. Peng, M. Xie, J. Xia, X. Chang, C. Zou, W. Lu, *Inorg. Chem.* **2023**, *62*, 10077–10091.
[36] G. Y. Zheng, D. P. Rillema, *Inorg. Chem.* **1998**, *37*, 1392–1397.
[37] Y.-H. Chen, J. W. Merkert, Z. Murtaza, C. Woods, D. P. Rillema, *Inorg. Chim. Acta* **1995**, *240*, 41–47.
[38] J. Forniés, S. Fuertes, J. A. López, A. Martín, V. Sicilia, *Inorg. Chem.* **2008**, *47*, 7166–7176.
[39] B. D. Belviso, F. Marin, S. Fuertes, V. Sicilia, R. Rizzi, F. Ciriaco, C. Cappuccino, E. Dooryhee, A. Falcicchio, L. Maini, A. Altomare, R. Caliandro, *Inorg. Chem.* **2021**, *60*, 6349–6366.
[40] T. Saito, M. Yoshida, K. Segawa, D. Saito, J. Takayama, S. Hiura, A. Murayama, N. M. Lakshan, W. M. C. Sameera, A. Kobayashi, M. Kato, *Chem. Sci.* **2024**, *15*, 14497–14505.
[41] Á. Díez, J. Forniés, C. Larraz, E. Lalinde, J. A. López, A. Martín, M. T. Moreno, V. Sicilia, *Inorg. Chem.* **2010**, *49*, 3239–3251.
[42] M. Martínez-Junquera, E. Lalinde, M. T. Moreno, *Inorg. Chem.* **2022**, *61*, 10898–10914.
[43] J. Forniés, V. Sicilia, P. Borja, J. M. Casas, A. Díez, E. Lalinde, C. Larraz, A. Martín, M. T. Moreno, *Chem. Asian J.* **2012**, *7*, 2813–2823.
[44] M. Kimura, M. Yoshida, S. Fujii, A. Miura, K. Ueno, Y. Shigeta, A. Kobayashi, M. Kato, *Chem. Commun.* **2020**, *56*, 12989–12992.
[45] T. Mochizuki, M. Yoshida, A. Kobayashi, M. Kato, *Dalton Trans.* **2024**, *53*, 12064–12072.
[46] D. Gómez de Segura, E. Lalinde, M. T. Moreno, *Inorg. Chem.* **2022**, *61*, 20043–20056.
[47] B.-S. Su, Y.-C. Wei, W.-T. Chuang, S.-C. Weng, S.-F. Wang, D.-G. Chen, Z.-X. Huang, Y. Chi, P.-T. Chou, *J. Phys. Chem. Lett.* **2021**, *12*, 7482–7489.
[48] D. Saito, T. Ogawa, M. Yoshida, J. Takayama, S. Hiura, A. Murayama, A. Kobayashi, M. Kato, *Angew. Chem. Int. Ed.* **2020**, *59*, 18723–18730.
[49] K. Sasaki, D. Saito, M. Yoshida, F. Tanaka, A. Kobayashi, K. Sada, M. Kato, *Chem. Commun.* **2023**, *59*, 6745–6748.
[50] H.-K. Yip, L.-K. Cheng, K.-K. Cheung, C.-M. Che, *J. Chem. Soc. Dalton Trans.* **1993**, 2933–2938.
[51] R. Büchner, C. T. Cunningham, J. S. Field, R. J. Haines, D. R. McMillin, G. C. Summerton, *J. Chem. Soc. Dalton Trans.* **1999**, 711–717.
[52] J. S. Field, R. J. Haines, D. R. McMillin, G. C. Summerton, *J. Chem. Soc. Dalton Trans.* **2002**, 1369–1376.
[53] J. S. Field, J.-A. Gertenbach, R. J. Haines, L. P. Ledwaba, N. T. Mashapa, D. R. McMillin, O. Q. Munro, G. C. Summerton, *Dalton Trans.* **2003**, 1176–1180.
[54] J. S. Field, L. P. Ledwaba, O. Q. Munro, D. R. McMillin, *CrystEngComm* **2008**, *10*, 740–747.
[55] A. Kobayashi, S. Imada, Y. Shigeta, Y. Nagao, M. Yoshida, M. Kato, *J. Mater. Chem. C* **2019**, *7*, 14923–14931.
[56] Y. Nishiuchi, A. Takayama, T. Suzuki, K. Shinozaki, *Eur. J. Inorg. Chem.* **2011**, 1815–1823.
[57] V. V. Sivchik, E. V. Grachova, A. S. Melnikov, S. N. Smirnov, A. Y. Ivanov, P. Hirva, S. P. Tunik, I. O. Koshevoy, *Inorg. Chem.* **2016**, *55*, 3351–3363.
[58] Y. Chen, W. Lu, C.-M. Che, *Organometallics* **2013**, *32*, 350–353.
[59] D. Saito, K. Segawa, M. Kikkawa, M. Yoshida, A. Kobayashi, M. Kato, *Cryst. Growth Des.* **2024**, *24*, 7194–7201.
[60] N. Lu, L. M. Hight, D. R. McMillin, J.-W. Jhuo, W.-C. Chung, K.-Y. Lin, Y.-S. Wen, L.-K. Liu, *Dalton Trans.* **2014**, *43*, 2112–2119.
[61] Y. Makino, M. Yoshida, S. Hayashi, T. Sasaki, S. Takamizawa, A. Kobayashi, M. Kato, *Dalton Trans.* **2023**, *52*, 8864–8872.
[62] a) S. S. Batsanov, *Inorg. Mater.* **2001**, *37*, 871–885; b) S. Alvarez, *Dalton Trans.* **2013**, *42*, 8617–8636; c) N. Harris, A. K. Sakr, H. V. Snelling, N. A. Young, *J. Mol. Struct.* **2018**, *1172*, 80–88.
[63] T. Morimoto, M. Yoshida, A. Sato-Tomita, S. Nozawa, J. Takayama, S. Hiura, A. Murayama, A. Kobayashi, M. Kato, *Chem. Eur. J.* **2023**, *29*, e202301993.
[64] C.-W. Hsu, K. T. Ly, W.-K. Lee, C.-C. Wu, L.-C. Wu, J.-J. Lee, T.-C. Lin, S.-H. Liu, P.-T. Chou, G.-H. Lee, Y. Chi, *ACS Appl. Mater. Interfaces* **2016**, *8*, 33888–33898.
[65] K.-H. Kim, J.-L. Liao, S. W. Lee, B. Sim, C.-K. Moon, G.-H. Lee, H. J. Kim, Y. Chi, J.-J. Kim, *Adv. Mater.* **2016**, *28*, 2526–2532.
[66] W.-C. Chen, C. Sukpattanacharoen, W.-H. Chan, C.-C. Huang, H.-F. Hsu, D. Shen, W.-Y. Hung, N. Kungwan, D. Escudero, C.-S. Lee, Y. Chi, *Adv. Funct. Mater.* **2020**, *30*, 2002494.
[67] M. Chaaban, S. Lee, J. S. Raaj Vellore Winfred, X. Lin, B. Ma, *Small Structures* **2022**, *3*, 2200043.
[68] J. Forniés, N. Giménez, S. Ibáñez, E. Lalinde, A. Martín, M. T. Moreno, *Inorg. Chem.* **2015**, *54*, 4351–4363.
[69] J. Forniés, S. Ibáñez, E. Lalinde, A. Martín, M. T. Moreno, A. C. Tsipis, *Dalton Trans.* **2012**, *41*, 3439–3451.
[70] V. Phillips, F. G. Baddour, T. Lasanta, J. M. López-de-Luzuriaga, J. W. Bacon, J. A. Golen, A. L. Rheingold, L. H. Doerrer, *Inorg. Chim. Acta* **2010**, *364*, 195–204.
[71] J. K. Nagle, A. L. Balch, M. M. Olmstead, *J. Am. Chem. Soc.* **1988**, *110*, 319–321.
[72] D. Dalmau, E. P. Urriolabeitia, *Molecules* **2023**, *28*, 2663.
[73] Q. Wan, W.-P. To, C. Yang, C.-M. Che, *Angew. Chem. Int. Ed.* **2018**, *57*, 3089–3093.
[74] C. Zou, J. Lin, S. Suo, M. Xie, X. Chang, W. Lu, *Chem. Commun.* **2018**, *54*, 5319–5322.
[75] a) Q. Wan, W.-P. To, X. Chang, C.-M. Che, *Chem* **2020**, *6*, 945–967; b) Q. Wan, D. Li, J. Zou, T. Yan, R. Zhu, K. Xiao, S. Yue, X. Cui, Y. Weng, C.-M. Che, *Angew. Chem. Int. Ed.* **2022**, *61*, e202114323; c) Q. Wan, K. Xiao, Z. Li, J. Yang, J. T. Kim, X. Cui, C.-M. Che, *Adv. Mater.* **2022**, *34*, 2204839.
[76] a) J. Lin, C. Zou, X. Zhang, Q. Gao, S. Suo, Q. Zhuo, X. Chang, M. Xie, W. Lu, *Dalton Trans.* **2019**, *48*, 10417–10421; b) Ji. Lin, M. Xie, X. Zhang, Q. Gao, X. Chang, C. Zou, W. Lu, *Chem. Commun.* **2021**, *57*, 1627–1630; c) N. Zhou, C. Zou, S. Suo, Y. Liu, J. Lin, X. Zhang, M. Shi, X. Chang, W. Lu, *Dalton Trans.* **2023**, *52*, 5503–5513; d) N. Zhou, M. Xie, C. Zheng, J. An, C. Zou, W. Lu, *Adv. Opt. Mater.* **2024**, *12*, 2400295.
[77] a) S. C. Gangadharappa, I. Maisuls, M. E. Gutierrez Suburu, C. A. Strassert, *Z. Naturforsch. B* **2021**, *76*, 811–818; b) T. Theiss, S. Buss, I. Maisuls, R. López-Arteaga, D. Brünink, J. Kösters, A. Hepp, N. L. Doltsinis, E. A. Weiss, C. A. Strassert, *J. Am. Chem. Soc.* **2023**, *145*, 3937–3951.
[78] L. Cao, K. Klimes, Y. Ji, T. Fleetham, J. Li, *Nat. Photonics* **2021**, *15*, 230–237.
[79] M. V. Kashina, K. V. Luzyanin, D. V. Dar'in, S. I. Bezzubov, M. A. Kinzhalov, *Inorg. Chem.* **2024**, *63*, 5315–5319.
[80] a) Y. Ohashi, I. Hanazaki, S. Nagakura, *Inorg. Chem.* **1970**, *9*, 2551–2556; b) K. Takeda, T. Sasaki, J. Hayashi, S. Kagami, I. Shirotani, K. Yakushi, *J. Phys. Conf. Ser.* **2010**, *215*, 012065.

[81] M.-Y. Yuen, V. A. L. Roy, W. Lu, S. C. F. Kui, G. S. M. Tong, M.-H. So, S. S.-Y. Chui, M. Muccini, J. Q. Ning, S. J. Xu, C.-M. Che, *Angew. Chem. Int. Ed.* **2008**, *47*, 9895–9899.
[82] a) J. Li, X.-F. Zhu, L.-Y. Zhan, Z.-N. Chen, *RSC Adv.* **2015**, *5*, 34992–34998; b) L. M. C. Luong, M. A. Malwitz, V. Moshayedi, M. M. Olmstead, A. L. Balch, *J. Am. Chem. Soc.* **2020**, *142*, 5689–5701; c) M. Feng, F. Liu, N. Yang, Ji. Yu, W. Yang, D. J. Young, X.-Q. Cao, H.-X. Li, Z.-G. Ren, *Inorg. Chem.* **2023**, *62*, 6439–6446.
[83] a) F. Baril-Robert, M. A. Radtke, C. Reber, *J. Phys. Chem. C* **2012**, *116*, 2192–2197; b) A. J. Blake, R. Donamaría, V. Lippolis, J. M. López-de-Luzuriaga, M. Monge, M. E. Olmos, A. Seal, J. A. Weinstein, *Inorg. Chem.* **2019**, *58*, 4954–4961.
[84] M. Gao, W.-P. To, G. S. M. Tong, L. Du, K.-H. Low, Z. Tang, W. Lu, C.-M. Che, *Angew. Chem. Int. Ed.* **2025**, *64*, e202414411.
[85] a) R. Sekiya, Y. Tsutsui, W. Choi, T. Sakurai, S. Seki, Y. Bando, H. Maeda, *Chem. Commun.* **2014**, *50*, 10615–10618; b) T. Seki, K. Sakurada, M. Muromoto, S. Seki, H. Ito, *Chem. Eur. J.* **2016**, *22*, 1968–1978.

Manuscript received: November 28, 2024
Revised manuscript received: March 1, 2025
Accepted manuscript online: March 3, 2025
Version of record online: ■■, ■■

REVIEW

One-dimensional Pt(II) complexes are known to exhibit significant thermochromic emissions in the crystalline state. This phenomenon offers valuable insights into the excited states of Pt(II) complexes. This review focuses on the thermochromic mechanisms of one-dimensional Pt(II) and Pd(II) complexes from the viewpoint of the relationship between stacking structures and photophysical properties.

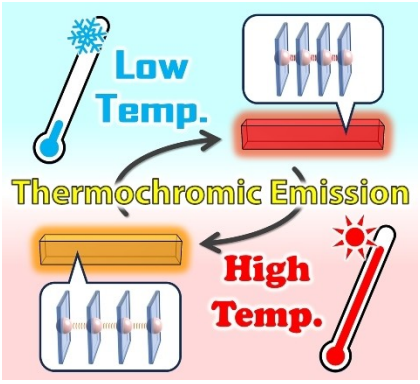

M. Yoshida, M. Kato**

VIP